

Zerong XING, Junheng FU, Sen CHEN, Jianye GAO, Ruiqi ZHAO, Jing LIU

Perspective on gallium-based room temperature liquid metal batteries

© Higher Education Press 2022

Abstract Recent years have witnessed a rapid development of deformable devices and epidermal electronics that are in urgent request for flexible batteries. The intrinsically soft and ductile conductive electrode materials can offer pivotal hints in extending the lifespan of devices under frequent deformation. Featuring inherent liquidity, metallicity, and biocompatibility, Ga-based room-temperature liquid metals (GBRTLMS) are potential candidates to fulfill the requirement of soft batteries. Herein, to illustrate the glamour of liquid components, high-temperature liquid metal batteries (HTLMBs) are briefly summarized from the aspects of principle, application, advantages, and drawbacks. Then, Ga-based liquid metals as main working electrodes in primary and secondary batteries are reviewed in terms of battery configurations, working mechanisms, and functions. Next, Ga-based liquid metals as auxiliary working electrodes in lithium and nonlithium batteries are also discussed, which work as functional self-healing additives to alleviate the degradation and enhance the durability and capacity of the battery system. After that, Ga-based liquid metals as interconnecting electrodes in multi-scenarios including photovoltaics solar cells, gen-

erators, and supercapacitors (SCs) are interpreted, respectively. The summary and perspective of Ga-based liquid metals as diverse battery materials are also focused on. Finally, it was suggested that tremendous endeavors are yet to be made in exploring the innovative battery chemistry, inherent reaction mechanism, and multifunctional integration of Ga-based liquid metal battery systems in the coming future.

Keywords liquid metals, soft electrodes, flexible batteries, deformable energy supply devices, epidermal electronics

1 Introduction

The current advancements in deformable devices such as wearable epidermal electronics, sensors, and soft robotic systems have given impetus to the exploration for flexible energy supply devices [1]. A pretty rapidly growing sector of energy economy is that of electrical energy generation [2–4], which is currently the most versatile and convenient form due to its high conversion efficiency and absence of gaseous exhausts [5]. Batteries, referring to the device that provides electric energy through electrochemical reaction in the traditional sense, are one of the most common and familiar electrical energy supply devices. Nevertheless, conventional rigid electrical batteries have emerged as a critical bottleneck for the development of deformable electronics [6]. Over the last decades, a series of emerging technologies such as multi-form nanogenerators [7,8], supercapacitors (SCs) [9,10], and photovoltaic solar cells [11–13] have also been exhaustingly studied for powering, which should not be overlooked. Herein, the concept of batteries is extended from electrochemical cells to electric supply devices to cater to technological developments.

To meet the requirements of deformable devices, meticulously designed structures and elaborately operated processes are explored for batteries. Generally, coating a thin layer of hard material onto an elastomeric substrate, or

Received Jun. 27, 2021; accepted Nov. 1, 2021; online Feb. 28, 2022

Zerong XING, Junheng FU
Technical Institute of Physics and Chemistry, Chinese Academy of Sciences, Beijing 100190, China; School of Future Technology, University of Chinese Academy of Sciences, Beijing 100049, China

Sen CHEN
School of Medicine, Tsinghua University, Beijing 100084, China

Jianye GAO, Ruiqi ZHAO
Technical Institute of Physics and Chemistry, Chinese Academy of Sciences, Beijing 100190, China; School of Engineering Science, University of Chinese Academy of Sciences, Beijing 100049, China

Jing LIU (✉)
Technical Institute of Physics and Chemistry, Chinese Academy of Sciences, Beijing 100190, China; School of Future Technology, University of Chinese Academy of Sciences, Beijing 100049, China; School of Medicine, Tsinghua University, Beijing 100084, China
E-mail: jliu@mail.ipc.ac.cn

connecting the hard material with a specially designed structure on a soft substrate are two universal strategies for flexible batteries. Structures like origami [14], kirigami [15], spring [16], serpentine [17], and island-bridge [18] have appeared in batteries. Complex fabrication processes like electron beam evaporation [17] and photolithography [14] usually set a high demand of time and investment. However, despite the delicateness of the structures and processes, the originally rigid materials cannot endure frequent deformation and movement. Only materials that are inherently flexible are perfectly suited for deformable devices.

Most metals and their alloys are solid at room temperature. Alkali metals and their alloys, mercury (Hg), and gallium (Ga) and their alloys, are in liquid state around ambient temperature (melting point $< 60^{\circ}\text{C}$). Alkali metals and their alloys are so active in air that they are not suitable for powering skin electronics. Hg is restricted because of the high toxicity and surface energy, while Ga and Ga-based room-temperature liquid metals (GBRTLMs), enumerated in Table 1, have shown sufficient stability in a natural environment and have been proven to have biocompatibility with human beings. GBRTLMs, with dual properties of metal and liquid, are emerging intriguing functional materials. They have recently been widely investigated in thermal management [23–28], flexible and reconfigurable electronics [29–32], microfluidic technology [33–36], soft robots [37–39], and biomedical engineering [40–42]. Moreover, GBRTLMs have been used in a variety of energy applications, including energy production [43–46], conversion [6,47,48], and storage [49–52]. They are competitive candidates for the realization of deformable batteries. Guo et al. [53] analyzed the design principles and relevant designs of easily fused metal- ($< 183^{\circ}\text{C}$) based batteries. Li et al. [54] reviewed recent research progresses of Hg, Ga, and In metals in Li, Na, K, and multi-valent metal batteries. Zhang et al. [55] summarized the remaining challenges and current progress of room-temperature liquid metal batteries from the aspects of wettability behavior, volume changes, and interface formation.

Nevertheless, GBRTLMs already have some applications as soft and self-healing electrodes in batteries which have not been systematically discussed. In this paper, the development process and characteristics of high-temperature liquid metal batteries (HTLMBs) are briefly reviewed to illustrate the attraction of liquid components and the limitations of HTLMBs. Subsequently, properties of GBRTLMs which enable them to be proper electrodes are summarized. Then the applications of GBRTLMs as electrodes are introduced in detail, classified as main reacting electrodes, auxiliary working electrodes, and interconnecting electrodes (Fig. 1). Additionally, the perspective of GBRTLMs is also outlined.

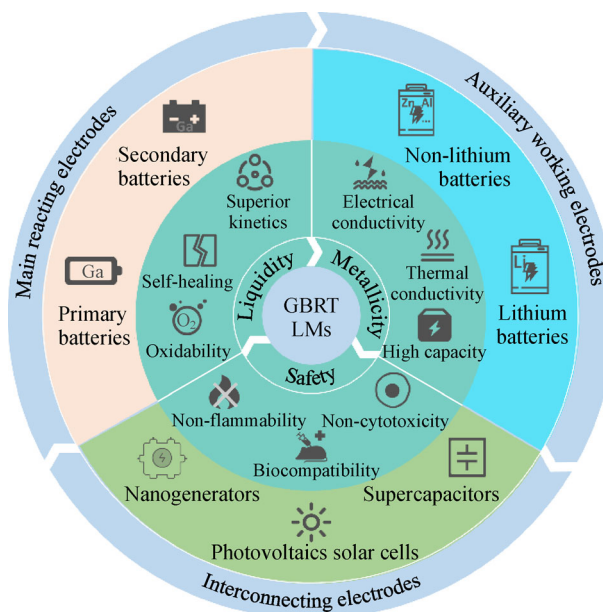


Fig. 1 Properties and applications of GBRTLMs in batteries.

2 Properties of liquid metal batteries

2.1 Development and properties of HTLMBs

The history of HTLMBs can be traced back to nearly a

Table 1 Room-temperature ($< 60^{\circ}\text{C}$) metal and alloys [19–22]

Metal/Alloy	Melting point/ $^{\circ}\text{C}$	Metal/Alloy	Melting point/ $^{\circ}\text{C}$
Ga	29.8	Ga _{62.5} In _{21.5} Sn ₁₆	10.7
Ga _{75.5} In _{24.5} (EGaIn)	15.4	Ga ₆₂ In ₂₅ Sn ₁₃	11
Ga _{86.5} Sn _{13.5}	20.5	Ga ₆₇ In ₂₉ Zn ₄	13
Ga ₈₈ Sn ₁₂	25	Ga ₇₂ In ₁₂ Zn ₁₆	17
Ga _{96.1} Zn _{3.9}	24.7	Ga ₆₁ In ₂₅ Sn ₁₃ Zn ₁	8
Ga _{97.6} Al _{2.4}	25.9	Bi _{32.5} In ₅₁ Sn _{16.5}	60
Ga _{96.4} Ag _{3.6}	26.0	Bi ₄₉ In ₂₁ Pb ₁₈ Sn ₁₂	58
Ga _{98.0} Hg _{2.0}	27.0	Bi ₃₅ In _{48.6} Sn ₁₆ Zn _{0.4}	58.3
Ga _{68.5} In _{21.5} Sn ₁₀ (Galinstan)	13.2	Bi _{44.7} Pb _{22.6} In _{19.1} Sn _{8.3} Cd _{5.3}	47

century ago when ultrahigh-purity Al was produced. Later, liquid metal batteries have experienced a long period of alternating development and halt until the widespread use of intermittent renewable energy [56,57] which has dramatically increased the demand for low-cost [58], long-lifespan, and grid-scale energy storage devices. Hence, liquid metal batteries once again received attention.

The HTLMBs consist of two liquid metal electrodes, the middle of which is separated by molten salt electrolyte. Due to different densities and immiscibility, the three layers are spontaneously self-segregated into the upper (negative electrode), middle, and bottom (positive electrode) layers. The strong interaction between two electrodes metals provides a thermodynamic driving force for liquid metal batteries. During discharging process, the negative metal is oxidized, and the layer thickness decreases. The oxidized metal ions pass through the molten salt electrolyte to form an alloy with the positive metal. At the same time, the thickness of the positive metal layer increases. The charging process is the opposite of discharging process (Fig. 2(a)). The candidates of the two electrodes are highlighted in Periodic Table [59] (Fig. 2(b)).

Since 2006, Massachusetts Institute of Technology (MIT) has restarted developing HTLMBs. A series of significant works have been reported [59–61]. Sodium-bismuth (Na||Bi) liquid metal battery were first tested with NaF-NaCl-NaI eutectic salt electrolytes at 560°C [59]. Limited by the comparatively higher self-discharge current and higher price of Bi, the researchers shifted their focus on magnesium-antimony (Mg||Sb) liquid metal batteries incorporating a molten salt NaCl-KCl-MgCl₂ electrolyte at 700°C (Fig. 2(c)) [60]. Subsequently, a lithium-antimony-lead (Li||Sb-Pb) liquid metal battery using molten lithium halide electrolyte LiF-LiCl-LiI with an operating temperature of about 450°C were studied [61]. Additionally, it was found that self-healing Li||Bi HTLMBs can be discharged deeper with a reversible solid intermetallic compound formed in the positive electrode. Three orders of magnitude prototype cells were assembled to demonstrate the novel self-healing concept as illustrated in Fig. 2(d) [62].

Further research into liquid metal batteries has focused on exploration of new battery chemistries [62–65], reasonable control of interfaces [66,67], efficient management of battery [68,69], and reduction in the operating

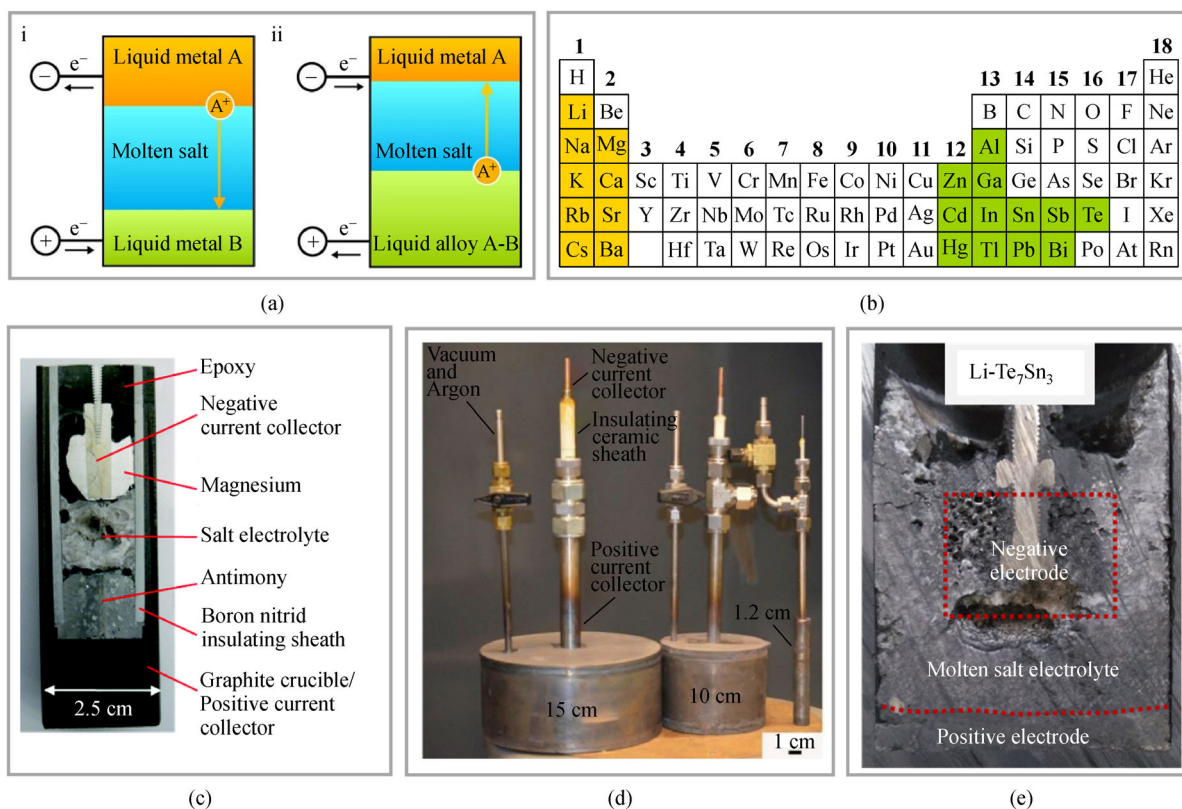


Fig. 2 Principles and examples of HTLMBs.

(a) Schematic diagram of HTLMBs under different conditions (i: discharging; ii: charging (adapted with permission from Ref. [59])); (b) negative (orange) and positive (green) electrodes material candidates for HTLMBs (adapted with permission from Ref. [59]); (c) sectioned Mg||Sb liquid metal battery operated at 700°C showing the three stratified liquid phases upon cooling to room temperature (adapted with permission from Ref. [60]); (d) cell schematic and optical image of self-healing Li||LiCl-LiF||Bi liquid metal battery (adapted with permission from Ref. [62]); (e) cross section of Li||Te₇Sn₃ cell cooled down at fully discharged state (adapted with permission from Ref. [65]).

temperature [70–72]. Li et al. [65] reported a battery employing alloyed tellurium-tin (Te-Sn) as positive electrode. The introduction of Sn not only enhanced the electronic conductivity of Te electrodes, but also suppressed the solubility of Te in molten salt electrolyte. The Li||Te-Sn cell presented a high discharge voltage and energy density (Fig. 2(e)).

Compared with presently available batteries, the specialties of HTLMBs can be attributed to performance, lifespan, cost, and application fields. In terms of performance, the liquidity of both electrodes and electrolytes endows an excellent kinetic. Regarding lifespan, all liquid active materials are unsusceptible to mechanical failures so that some degradation mechanisms such as volume expansion and dendrite growth can be avoided. In respect of cost, low-budget can be achieved through proper selection of materials which are earth-abundant and inexpensive. So far as application is concerned, liquid metals are sensitive to motion and have magneto hydrodynamic instabilities [73,74], which may cause short circuit. In other words, unlike other batteries which can be used in portable devices and flexible electronics, HTLMBs are only suitable for static energy storage. In addition, other disadvantages of HTLMBs such as the need for high temperature to ensure the molten state of the materials, and the resulting requirements for rigorous thermal management, hermetic seal, and stringent corrosion protection, are summarized in Table 2.

Table 2 Advantages and drawbacks of HTLMBs [2,59,73]

Advantages	Drawbacks
Excellent kinetics and transport properties	High temperature ($> 200^{\circ}\text{C}$)
Low cost	Low specific energy density ($> 200 \text{ W}\cdot\text{h}\cdot\text{kg}^{-1}$)
Simple assembly	Low equilibrium cell voltages ($< 1.0 \text{ V}$)
Long lifespan	Static storage
Grid level energy storage potential	Rigorous thermal management
–	Stringent corrosion protection
–	Hermetic-seal demand

Grid-level storage devices are not suitable for wearable applications. The low-cost and scalability are important for the former while the miniaturization and adaptability are more critical in the latter. GBRTLMBs are potential cathode material candidates in principle. Nevertheless, their relatively high market prices hinder their use in large-scale energy storage [20,59]. The utilization of GBRTLMBs can reduce the investment of thermal management, sealing, and corrosion protection. In this regard, they can be attractive candidates for smaller device designs where thermal management is critical [75]. On the other hand, the flexibility and stretchability make them suitable as energy supply devices for bendable wearable devices [76]. The

main source of Ga is the by-product of the extraction of other metals. Therefore, the price of Ga is volatile, depending on the market of the main products. The preponderance of the relatively high crustal abundance, which is smaller than that of Li, comparable with copper (Cu) and nickel (Ni), and larger than cobalt (Co) [77], indicates the potential great supply and low cost in the future [76]. Additionally, the cost can be further reduced by alloying Ga with cheaper metals such as Sn. Besides, Ga-Sn alloy-based electrode is demonstrated to have comparable electrochemical performance [76].

2.2 Properties of gallium-based liquid metals

2.2.1 Liquidity

Post transition metals with low melting and high boiling points are at a liquid state over a wide temperature range, among which gallium has a melting point of 29.8°C and a high boiling point of 2403°C [20]. The low melting point of gallium attributes to the weak binding of atoms, which is induced by the relatively large interatomic distance. This facilitates the breakup of crystal structure at a low temperature compared to most metals [20]. The melting point can be tuned by introducing other metallic elements like In, Sn, and so on, which causes disordered structure and broadens the atomic distance between metallic atoms [78]. Through adjusting the composition according to the temperature demand, the alloy method makes the extensive application scenarios in a wider range of temperature possible [79]. $\text{Ga}_{75.5}\text{In}_{24.5}$ (EGaIn) and $\text{Ga}_{68.5}\text{In}_{21.5}\text{Sn}_{10}$ (Galinstan), having a melting point of 15.4°C [80] and 13.2°C , respectively [20], are two typical alloys that are most studied. Besides, GBRTLMBs exhibits a strong tendency to be supercooled below the melting point [48,81]. It is worth noting that Galinstan will not freeze until -19°C due to supercooling which is different from melting [20].

Liquidity has a series of advantages such as storage convenience [50], unprecedented lifespan, and superior kinetics transport [59]. However, GBRTLMBs possess extraordinary surface tension which is approximately 7–10 times larger than that of water [48]. Because of this, they tend to agglomerate into a sphere, greatly reducing the effective surface area of the electrode. Nevertheless, just because of the large surface tension, GBRTLMBs are one of the best candidates as functional battery materials to realize self-healing [5] and the ability to repair damage [82]. Liquid metal electrodes can return to liquid state even after experiencing a solid mesophase during the reaction. As soon as the liquid phase forms, the liquid metal droplets will merge. This feature is enamored by batteries because the rapid development of deformable devices has put forward unprecedented mechanical stretchability requirements. Self-healing would significantly avoid the battery

failure induced by large volume change such as fracture and crack formation, thus improving the lifespan, durability, and safety of devices [83].

Liquid gallium can also behave in a completely different solid-like way [84]. As soon as gallium contacts with oxygen, a concentration even as low as a few ppm is sufficient [20], and a passive layer composed of gallium oxides with a thickness of 0.5–3 nm [84,85] forms on the surface. The oxide layer skin will be easily dissolved by acidic or alkaline solutions. It was established that about 0.2 V of the total polarization could be attributed to the drop in voltage across a suddenly formed passive layer on the surface of the gallium [50]. The presence of this skin totally changes the viscosity, surface tension, contact angle, and wetting behavior [86] of GBRTLMS, among which wetting behavior is also an important issue in the batteries. The rapid electrochemical reaction of the batteries requires a good contact between the collector, reactive materials, and electrolyte. The skin facilitates the adherence of GBRTLMS with surrounding environment and enables liquid metals to be patterned in arbitrary shapes [87], making it possible for GBRTLMS to be freestanding electrodes in all sorts of substrates [88].

2.2.2 Metallicity

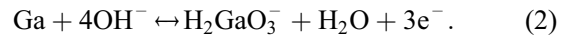
Metals can be in both solid and liquid states because metallic bonds exhibit a low directionality. Metallic atoms are less electronegative and tend to lose electrons. This means that the outermost electrons are easily separated from the atom, and the electron-deprived atom is immersed in a “cloud” or “sea” of electrons shared by each atom. The liquid metal and the solid metal are different in that the atoms of the liquid metal can also move [20]. Theoretical research on the eutectic alloy Galinstan have been conducted. The results showed that most of the density of free electrons exists around Ga atoms, thus the conclusion could be drawn that the conduction is mainly centered on Ga atoms [78]. The electrical conductivity of GBRTLMS is approximately 3.4×10^6 S/m at 295 K, an order of magnitude lower than Cu and orders of magnitude larger than most liquids [89,90]. In epidermal electronics, the thickness of circuit should be extremely thin (< 10 μm) to make conformability possible and reduce the strain applied to the devices or modulus [91]. A series of methods have been developed to patterned GBRTLMS at a high-resolution, such as spraying [92,93], screen-printing [94], transfer printing [95], and GBRTLMS-polymer ink preparing [96,97]. The resistivity of patterned GBRTLMS with different thicknesses can be calculated according to the resistance calculation formula [89]

$$R = \frac{\rho l}{A}, \quad (1)$$

where R is the resistance, l is the length of the patterned

GBRTLMS, and A is the cross-sectional area. For GBRTLMS patterned with different thickness, the variation in resistance is mainly due to the influence of cross-sectional areas. When the width and the length are constant, the resistance is proportional to the reciprocal of the thickness. The experimental results indicated that the resistance of a 100 μm wide and 50 μm thick liquid metal line had a resistance of about 1 Ω [93]. It can be roughly estimated that the resistance decreases to about 0.5 Ω as the thickness increases to 100 μm and to 5 Ω as the thickness decreases to 10 μm . GBRTLMS can maintain a superb metallic conductivity while meeting the thickness requirements of flexible electronics. Hence, when flexibility and adaptability is of utmost importance such as epidermal electronics [98], it is time for GBRTLMS to appear on the stage. Like ordinary metals, GBRTLMS also exhibit an excellent thermal conductivity. For example, Ga has a thermal conductivity of 29.8 W/(m·K) of over 40 times higher than that of water (0.599 W/(m·K)) at 20°C [99].

The metallicity of liquid metals allows them to dissolve most metal elements at relatively high concentrations [20]. As a result, they can be applied as reaction media for metal batteries [75,100]. Taking Li as an example, when Ga is fully embedded with Li, per Ga atom hosting 2 Li atoms, Li_2Ga alloy will be formed with a theoretical capacity of 769 mA·h/g [101], showing a discharge potential close to the Li/Li⁺ reaction [75]. From electrochemical aspect, Ga has a relatively negative standard reference voltage of about -1.22 V versus standard hydrogen electrode (SHE) for the equilibrium [50]



Although Ga has a low equivalent weight of 23 g/F, another property that is noticeable is the high polarization of Ga relative to hydrogen [102], leading to its high corrosion resistance. Pure Ga does not corrode easily, and the corrosion rate is low even at high temperatures. It is measured that the amount of Ga that dissolves corresponding to a corrosion current is about 8 mA/cm² in 6 mol/L of KOH solution without flow of current [50].

2.2.3 Safety

Safety is always of the utmost importance when powering flexible epidermal electronics. Alkali metals have been extensively studied in batteries. However, there are inevitably a series of safety problems, such as thermal runaway, dendrite formation, and inflation, which may occur instantaneously and cause catastrophic safety accidents [103]. For example, Li metal is an attractive anode, but its practical application has been prevented by the uncontrollable dendrite formation over 40 years [104]. Unlike alkali metals, GBRTLMS generally are biologically safe [105] and own a very small vapor pressure ($< 10^{-6}$ Pa at 500°C [106]). It was experimentally verified that

GBRTLMS did not have a general cytotoxicity [107,108] and biotoxicity [106,109]. In addition, a growing number of experiments have been conducted *in vivo* and *in vitro* to show the good biocompatibility of GBRTLMS [41,42,105,110–112]. Moreover, GBRTLMS are stable and nonflammable in air. These features make GBRTLMS very convenient to be handled.

It is worth noting that the contact of GBRTLMS can cause severe embrittlement in normally ductile solid metals, such as Al and Cu [113]. The chemical reaction between the Ga-In eutectic alloy with Al and the Al-base alloy have been studied [114]. The experimental results show that liquid metal diffuses on the surface, grain-boundary, and volume of Al. The surface diffusion destroys the oxide film and reduces the surface energy of Al. The grain-boundary diffusion and volume diffusion cause the change of composition in Al and lead to embrittlement [114,115], which has been exploited to achieve instant hydrogen production [116,117] for hydrogen fuel cells. Nevertheless, when GBRTLMS are designed as the electrode, the structural material of the battery should be properly screened to avoid corrosion.

With an intrinsically excellent liquidity and metallicity, adequate safety, relatively negative standard reference voltage, self-healing capability, and ability to be patterned in arbitrary shape, GBRTLMS have the potential to be flexible electrodes in batteries.

3 Gallium-based liquid metals in batteries

3.1 Gallium-based liquid metals as main reacting electrodes in batteries

At this stage, GBRTLMS as main reacting components in

batteries have not been widely explored. In this part, several existing studies, listed in Table 3, are summarized and discussed in terms of battery configurations, working mechanisms, and battery functions. Further, there are also proposed candidates in patents to realize various prototyped room temperature liquid metal batteries for industrial trials [118,119].

3.1.1 Battery configurations

Designing of electrodes, electrolyte, and cell structure are three key elements of battery configuration. When GBRTLMS are designed as the main reacting electrodes, several issues need to be carefully addressed, including melting point, surface tension, density, and reacting rate. The melting point of pure Ga is slightly higher than room temperature which is not convenient for experiment and application. Thus, Ga-based alloys with lower melting points such as GaIn₁₀ [120], Ga_{75.5}In_{24.5} [121], and Ga_{68.5}In_{21.5}Sn₁₀ [51] are usually used as the main reacting liquid electrodes. There are several advantages when other metallic elements are introduced. It maintains the electrodes in the liquid state, enhances the capacity [122], and inhibits the corrosion of Ga in electrolyte due to the high hydrogen evolution over potential [120]. Moreover, the cost of electrodes can be reduced by introducing cheaper elements [76]. The high surface tension and density of GBRTLMS are another two key impediments. To decrease the surface tension, functional additives [123] and special structural designs [51,120,121] have been explored. It is proved that calcium chloride (CaCl₂) additives (Fig. 3(a)) can improve the interface reaction activity, thus enhancing battery performance [123]. Unique structure such as Cu-coated carbon fibers is prepared to avoid the influence of surface tension as depicted in Fig. 3(b) [51]. This structure

Table 3 GBRTLMS as main reacting electrodes in batteries

Year	Anode material	Cathode material	Electrolyte	OCP/V	Main functionalities	Rechargeability	Ref.
1963	Ga	Porous silver	6 mol/L KOH	1.0	–	No	[50]
1963	Ga	NiO	6 mol/L KOH	1.4	–	Yes	[50]
2017	Ga	Conductive gel	0.3 mol/L KOH	1.1	Flexible; 3D printing	No	[126]
2018	GaIn ₁₀	Carbon fiber yarn@Pt	PAA-based KOH	1.87	Elastic; renewable anode; current controlled	No	[120]
2019	Ga ₇₅ In ₂₅	MnO ₂	KOH/PAAm LiOH/KOH/PAAm	1.47	Stretchable	Yes	[123]
2020	Na _{54.1} K _{45.9}	Ga _{78.6} In _{21.4} Ga _{87.6} Sn _{12.4} Ga _{68.5} In _{21.5} Sn ₁₀	NaClO ₄ /DME/FEC KPF ₆ /DME/FEC	1	Facile fabrication; high safety	Yes	[76]
2021	Ga _{68.5} In _{21.5} Sn ₁₀ modified carbon fibers	Air electrodes	Filter paper (NaOH)	1.12	Flexibility; sensing; signal conversion	No	[51]
2021	Ga-foam	Carbon air electrode	Saturated NaCl	1.35	Lightweight; porous anode	No	[121]
2021	Ga ₆₈ In ₂₂ Sn ₁₀	PANI	GaCl ₃ /NH ₄ Cl/PVA	1.6	Shape-variable	Yes	[127]

Notes: OCP (open circuit potential); PAA (poly(acrylic acid)); PAAm (polyacrylamide); DME (dimethoxyethane); FEC (fluoroethylene carbonate); PVA (poly(vinyl alcohol)).

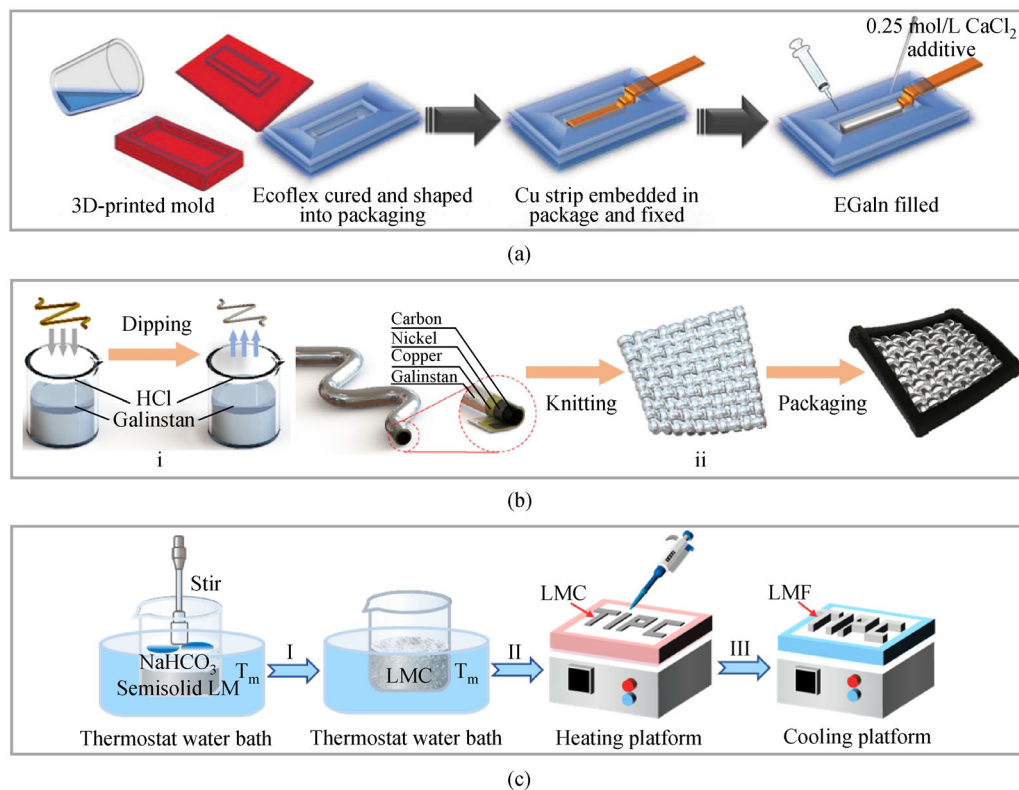


Fig. 3 Schematic diagrams of GBRTLMS anodes fabrication processes.

(a) EGaIn anode fabrication process with CaCl_2 additive to improve interface reaction activity (adapted with permission from Ref. [123]); (b) schematic illustration of preparing the Galinstan modified carbon fibers (G-CFs) anode (i: fabricating of G-CFs; ii: G-CFs line were knitted into a piece of fabrics whose four edges of the fabric were sealed to form the Galinstan anode (adapted with permission from Ref. [51]); (c) preparation process of Ga foam anode (adapted with permission from Ref. [121]).

combines the intermetallic alloying method to realize a better physical wetting of GBRTLMS and carbon fibers. The GBRTLMS are finally successfully dispersed on the supported substrate with a large superficial area to increase the active electrode area. To overcome the limitation caused by the high density and macroscopic interface of GBRTLMS, Gao et al. [121] introduced decomposition agent alkali bicarbonate to foam them. The preparation process of liquid metal foam (LMF) anode is illustrated in Fig. 3(c). The Ga is kept in a semisolid state by placing it in a thermostat water bath at a temperature slightly above the melting point of Ga. Then, NaHCO_3 particles are stirred into the beaker. Ga and NaHCO_3 composites (LMC) are placed on the heating platform, and the foaming process of LMF is based on the thermal decomposition reaction of NaHCO_3 particles. In GBRTLMS-air cells, the reaction rate of the cathode is usually limited. To improve the oxygen reduction reaction rate of the cathode, classical catalysts, such as Pt [120] and MnO_2 [124], are usually incorporated. Liu et al. [120] coated a thin layer of Pt nanoflowers array on the surface of the carbon fiber yarn by using the electrodeposition method to fabricate cathode electrode. This electrode enhanced the discharge performance of the battery by about 1.5 times, with a power density of

0.383 mW/cm^2 at 1.5 V.

The properties of GBRTLMS make the requirements of electrolyte both loose and rigorous. The loose property can be attributed to the liquid state which allows it to be molded into any shape, so the electrolyte can be filter paper [51], hydrogel [120,123] or any other forms as needed. It is rigorous because the easily formed passive skin on the surface of the GBRTLMS need to be removed in the electrolyte otherwise it will hinder the reaction. Therefore, most of the studies conducted have used the alkali solution as electrolyte [51,120,121]. Moreover, with a lower donor strength than water, the ionic liquid 1-butyl-3-methylimidazolium bis(trifluoromethylsulfonyl)imide ([BMIM][TFSI]) has also been explored to shift the redox potential window [52]. The ionic liquid can stabilize charged species by effectively shielding charges [125].

The utilization of GBRTLMS as electrodes do not have much restriction on the structure of batteries. Both sandwich-shaped (Figs. 4(a), 4(b), 4(d)) [51,121,123], 3D-printed (Fig. 4(c)) [126], and the cable-shaped (Fig. 4(e)) [120] batteries were constructed and demonstrated to be feasible. Poly(dimethylsiloxane) (PDMS), polyvinyl Chloride (PVC) tape, and thermoplastic polyurethane

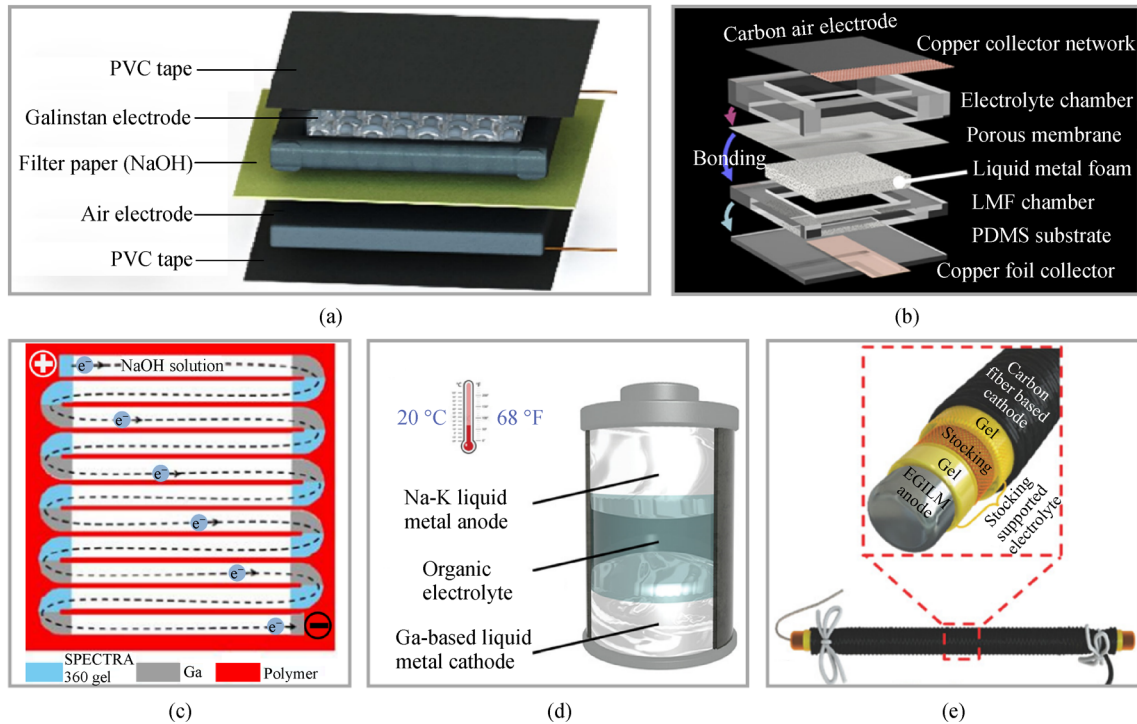


Fig. 4 Assorted structures of GBRTLMs based batteries.

(a) Composition of sandwich-shaped GBRTLM-air battery (adapted with permission from Ref. [51]); (b) structure of sandwich-shaped GBRTLM foam-air battery (adapted with permission from Ref. [121]); (c) schematic for 3D-printed GBRTLM battery where the dotted line indicates the migration of electrons inside batteries during charging process (adapted with permission from Ref. [126]); (d) configuration of sandwich-shaped room-temperature liquid metal battery (adapted with permission from Ref. [76]); (e) internal structure of cable-shaped GBRTLM-air battery (adapted with permission from Ref. [120]).

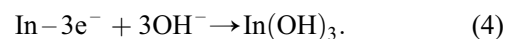
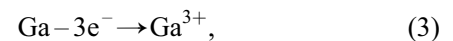
(TPU) were used as packaging materials in these studies. Using a Na-K alloy anode and a Ga-based alloy cathode as shown in Fig. 4(d), working in a similar way to HTLMBs, the all-liquid metal battery can be operated at room temperature. The temperature can even drop to -13°C when using Galinstan as cathode [76]. Recently, a shape-variable secondary liquid metal battery is developed using $\text{Ga}_{68}\text{In}_{22}\text{Sn}_{10}$ as liquid anode and a conductive polymer polyaniline (PANI) as cathode [127]. The battery can be deformed with a several millinewtons force without any capacity loss and realize a shape-adjustable battery construction among 1-D fiber, 2-D sheet, and 3-D spherical.

3.1.2 Working mechanisms

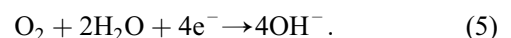
GBRTLMs as main reaction electrodes have been researched in both primary and secondary batteries. In the GBRTLMs-air galvanic cell, the GBRTLMs act as the negative electrode and lose electrons to be oxidized, while the oxygen in the air gains electrons to be reduced. The existing several works basically adopt such a principle [50,51,120,121]. Liu et al. [120] clearly elucidated this process using experiments, energy dispersive X-ray spectroscopy (EDS), and X-ray diffraction (XRD)

(Fig. 5(a)). They assembled an open-ended battery with GaIn_{10} as the anode and Pt coated carbon fiber yarn as the cathode in a glass beaker with 37.5% KOH solution as electrolyte. Three products, indium, $\text{In}(\text{OH})_3$, and GaOOH were found at the bottom of the beaker after one week of short-circuit current discharge. This meant all the Ga and a portion of the In participated in the discharge reaction and the remainder of the In was solidified into an In metal block. Hence, the working mechanism included five reactions, elaborately illustrated in Figs. 5(b)–5(c) [120]. The effective reactions in the anode and cathode are,

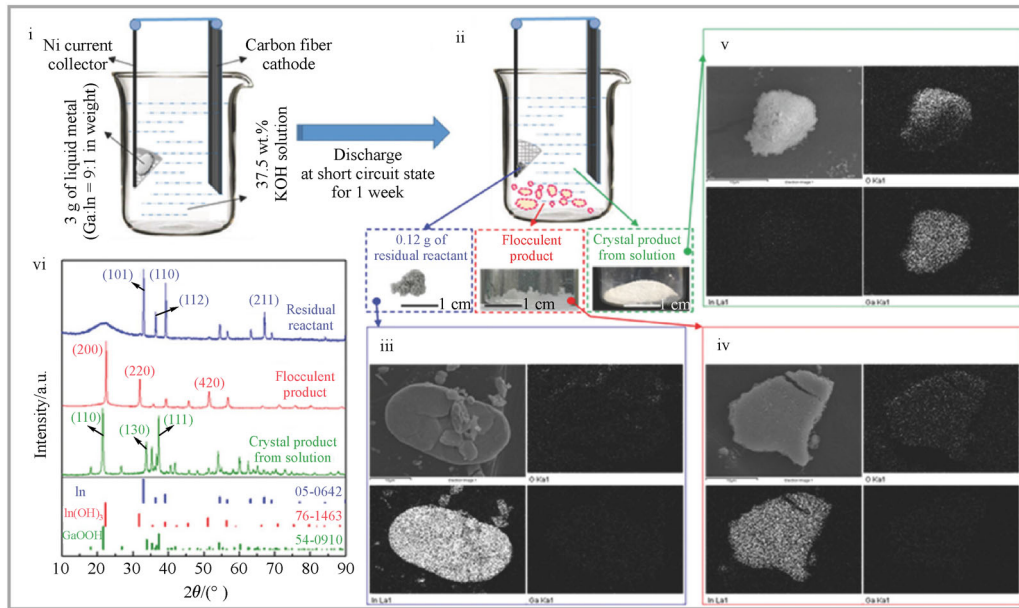
Anode:



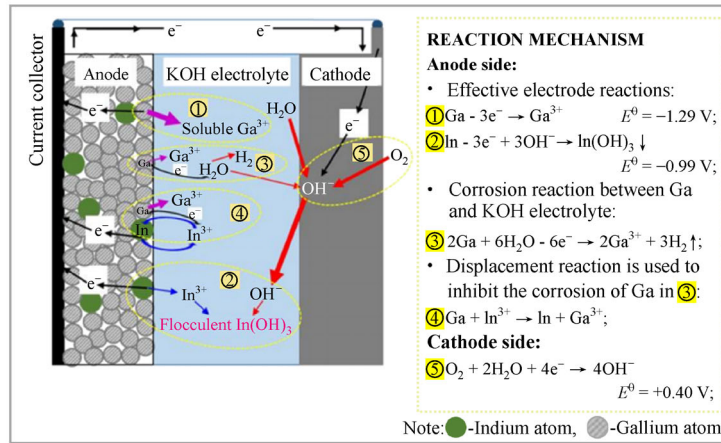
Cathode:



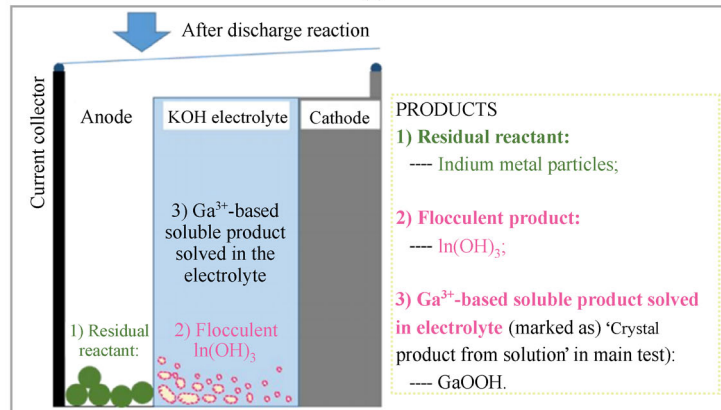
GBRTLMs can be used as either anodes or cathodes in secondary batteries. When used as positive electrodes, GBRTLMs mainly matched with the metal with higher activity, such as Li [72,75,128] and Na-K [76] alloy, based on the principle of HTLMBs. When used as negative



(a)



(b)



(c)

Fig. 5 Working mechanism of GaIn_{10} -air primary battery.

(a) Research of working mechanism through experiments and energy dispersive X-ray spectroscopy (EDS) (i: sketch of a beaker-type battery with GaIn_{10} anode, Ni current collector, carbon fiber cathode, and a 37.5% KOH (mass fraction) aqueous electrolyte; ii: sketch and photos; iii-v: element mappings; vi: XRD curves of the products after one week of discharge reaction); (b) sketch of working mechanism; (c) sketch of products of the liquid metal-air battery (adapted with permission from Ref. [120]).

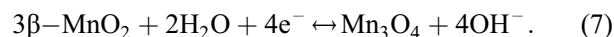
electrodes, the batteries operate via a hybrid mechanism of stripping and plating of Ga^{3+} and transformation reaction of paired electrodes such as Cl^- [127] and MnO_2 [123]. Liu and his coworkers [123] constructed a rechargeable battery system using $\text{Ga}_{75}\text{In}_{25}$ anode and MnO_2 cathode and analyzed the working mechanism (Figs. 6(a), 6(b)) of the rechargeable battery system through calculation and testing. Specifically, EDS mapping for the anode reactants in four states were taken respectively, including the pristine state, the state after the first discharging process, the state after first charging process, and the state after 100 discharge-charge cycles (Fig. 6(c)). The rechargeability of battery was accomplished through a mechanism that

involved reversible stripping and plating of gallium along with MnO_2 chemical conversion.

Anode:



Cathode:



GBRMLMs as the main reaction anode electrodes material in rechargeable batteries have not been exhaustingly explored, such as the selection of matching electrodes, suitable electrolyte, and rechargeable chemistries.

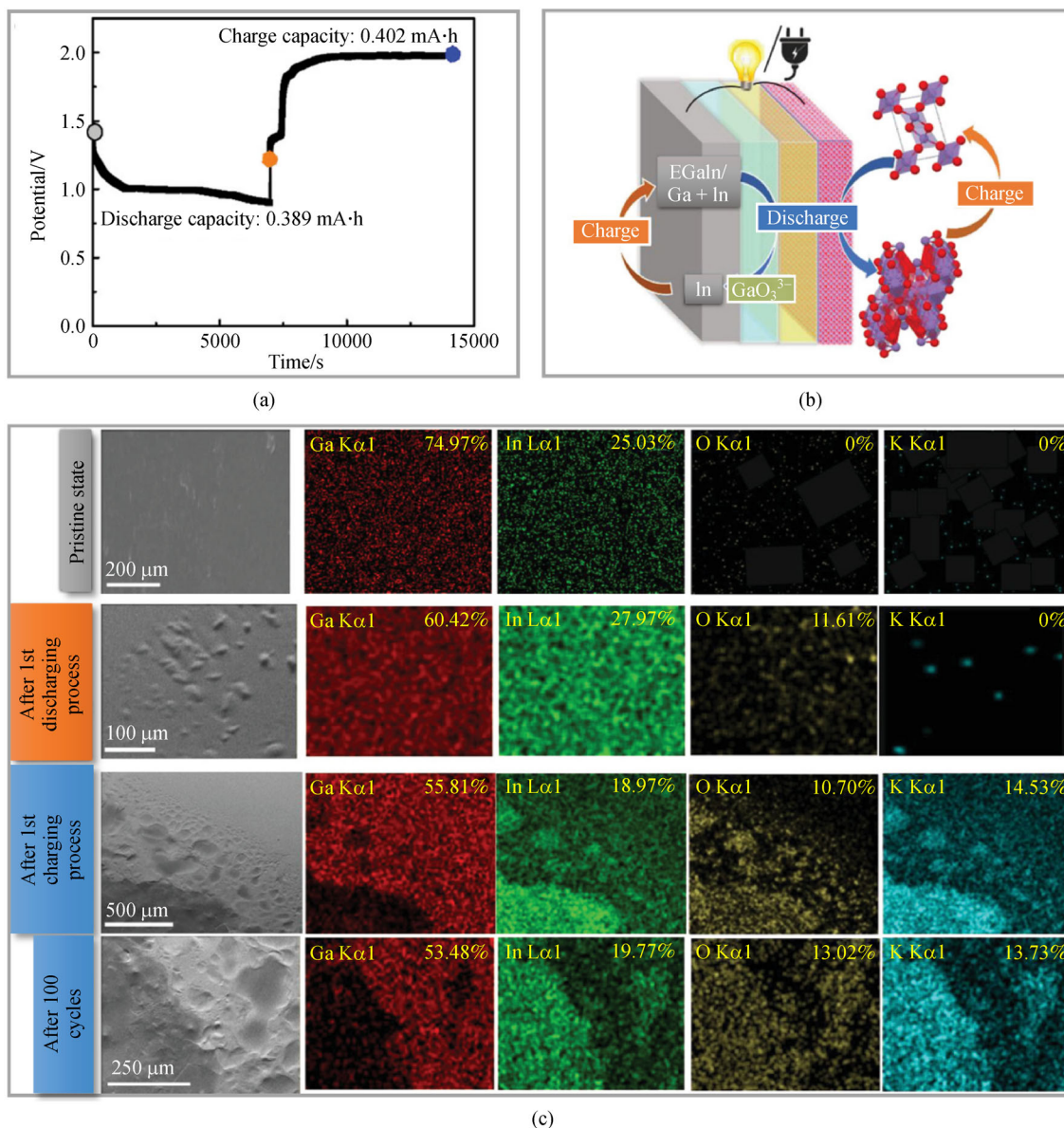


Fig. 6 Working mechanism of $\text{Ga}_{75}\text{In}_{25}\text{-MnO}_2$ secondary battery.

(a) Discharge and charge cycle for mechanism characterization; (b) schematic of electrochemical reaction for both electrodes; (c) scanning electron microscope (SEM) and EDS mapping results for the EGaIn anode in its pristine state, after the first discharging process, after the first charging process, and in the charged state after 100 discharge-charge cycles (adapted with permission from Ref. [123]).

3.1.3 Battery functions

GBRTLMS based batteries are supplement to the vacancy of HTLMBs in the field of portable devices and epidermal electronics. Wearable devices are required to deform smoothly with the body. Utilizing $\text{Ga}_{75}\text{In}_{25}$ and MnO_2 as anode and cathode, alkaline hydrogel as electrolyte, and soft elastomer as package, an all-soft stretchable battery was constructed [123]. The battery is highly flexible with a stretchability of up to 100% tensile strain and a bending radius of less than 2 mm without obvious structural damage. In practical application, the battery can continuously power an light emitting diode (LED) under a dynamic loading and a strain gauge while being attached and stretched on skin (Fig. 7(a)). The liquidity of GBRTLMS electrode endows the battery more unique properties. It can be a renewal anode simply with a syringe injecting and extracting. The discharge current can be easily controlled by adjusting the amount of GBRTLMS or the applied pressure of finger (Fig. 7(b)) [120]. In addition, the GBRTLMS-based batteries have the potential to be deformable energy devices at low temperatures and demanding environments [76,127]. Fu et al. [127] reported that a GBRTLMS-based battery delivered a capacity of 67.8 mA·h/g at 0.2 A/g with 100% of elasticity at approximately -5°C .

Gallium-based liquid metals have also been extensively studied in printed flexible circuits such as the DIY “Christmas tree” in Fig. 8(a). This feature can also be combined with flexible batteries to achieve fully flexible integrated systems. Additionally, with the further efforts of scholars, multiple functions like signal transducing and sensing have also been further integrated into GBRTLM battery as illustrated in Fig. 8(b) [51]. The humidity is converted into low and high-potential signals. Only when the humidity goes beyond the set threshold, will the digital switch turn the LED light on. The sensing function is achieved by the different responses of batteries to ethyl alcohol, methyl alcohol, and deionized water (DI) water, which is enabled by the sensitivity of Ga oxide layer. Devices integrated with energy storage, signal conversion, and sensing may have great potentials in the field of flexible electronics to realize all-in-one design [91].

3.2 Gallium-based liquid metals as auxiliary working electrodes in batteries

Having superior theoretical energy densities, electrochemically active metal anodes such as Li and Na have aroused much interest in development of advanced rechargeable batteries [129]. However, the failure mechanisms (Fig. 9(a)), including the growth and decomposition of solid electrolyte interface (SEI), separation of active material and collector, particle fracture and isolation, and random growth of dendrites need to be analyzed and

solved [129,130]. A great deal of effort has been made to increase the safety of batteries. Just like the autonomous ability of positive feedback regulation biological system, researchers have dedicated for the autonomous materials for battery systems. Controllable release of microencapsulated functional additives and integration of self-healing interlayers are two effective methods [130]. Just as listed in Table 4, GBRTLMS have been widely studied and utilized in lithium and non-lithium batteries as self-healing auxiliary electrodes.

3.2.1 Lithium batteries

Lithium metal is a prospective anode owing to its low density (0.59 g/cm^3), high theoretical specific capacity ($3860 \text{ mA}\cdot\text{h/g}$) and lowest negative electrochemical potential (-3.04 V versus SHE) [131,132]. However, Li-metal has such a high chemical reactivity that a series of problems have yet to be solved such as uncontrollable growth of Li dendrites and huge volume expansion. Metallic substrate can regulate Li deposition behaviors to inhibit the dendrite growth [133]. GBRTLMS such as Ga [131], GaSn [134], and GaInSnZn [135–137] have been used in lithium metal batteries (LMBs) and lithium-ion batteries (LIBs) to realize multifunctional regulation owing to their self-healing abilities [100,138]. As can be seen from the phase diagram [139] in Fig. 9(b)-i, the process of lithiation will lead to a rapid solidification of Ga. The phase diagram illustrates the preferred phase of Li-Ga alloy at different compositions at room temperature [53]. In the charging and discharging cycle at 40°C , as shown in Fig. 9(b)-ii, multiple voltage plateaus corresponding to the phase diagram of the intermetallic Li_2Ga_7 , LiGa, and Li_2Ga are formed. Deshpande et al. observed that the cracks of the metal could be repaired after complete delithiation [75], thus achieving self-healing. By means of being coated onto current collector, Li metal surface, and Mxene framework, GBRTLMS are demonstrated to regulate the nucleation barrier and thus realize isotropic Li deposition, stable C layer formation, and higher Li^+ diffusion coefficient (Fig. 9(c)) [131,134–137].

Si [140], Ge [141], and Sn [142] are promising anode materials for LIBs whose theoretical capacities are several times larger than those of the commercially used graphite ($372 \text{ mA}\cdot\text{h/g}$) negative electrode. However, they suffer from the short cycle life induced by volume expansion and contraction during the charging and discharging process [75]. GaInSn liquid alloy was utilized to spontaneously repair Si anode for Li-ion battery [143]. It was found that the mechanical stress induced by volume change could be absorbed by GBRTLMS. In addition, the fluidity of liquid metal ensured the eternal contact between Si and conducting network. Luo et al. [101] have studied the self-healing behavior of Ga thin film as an anode material for LIB in liquid electrolyte. The experimental results

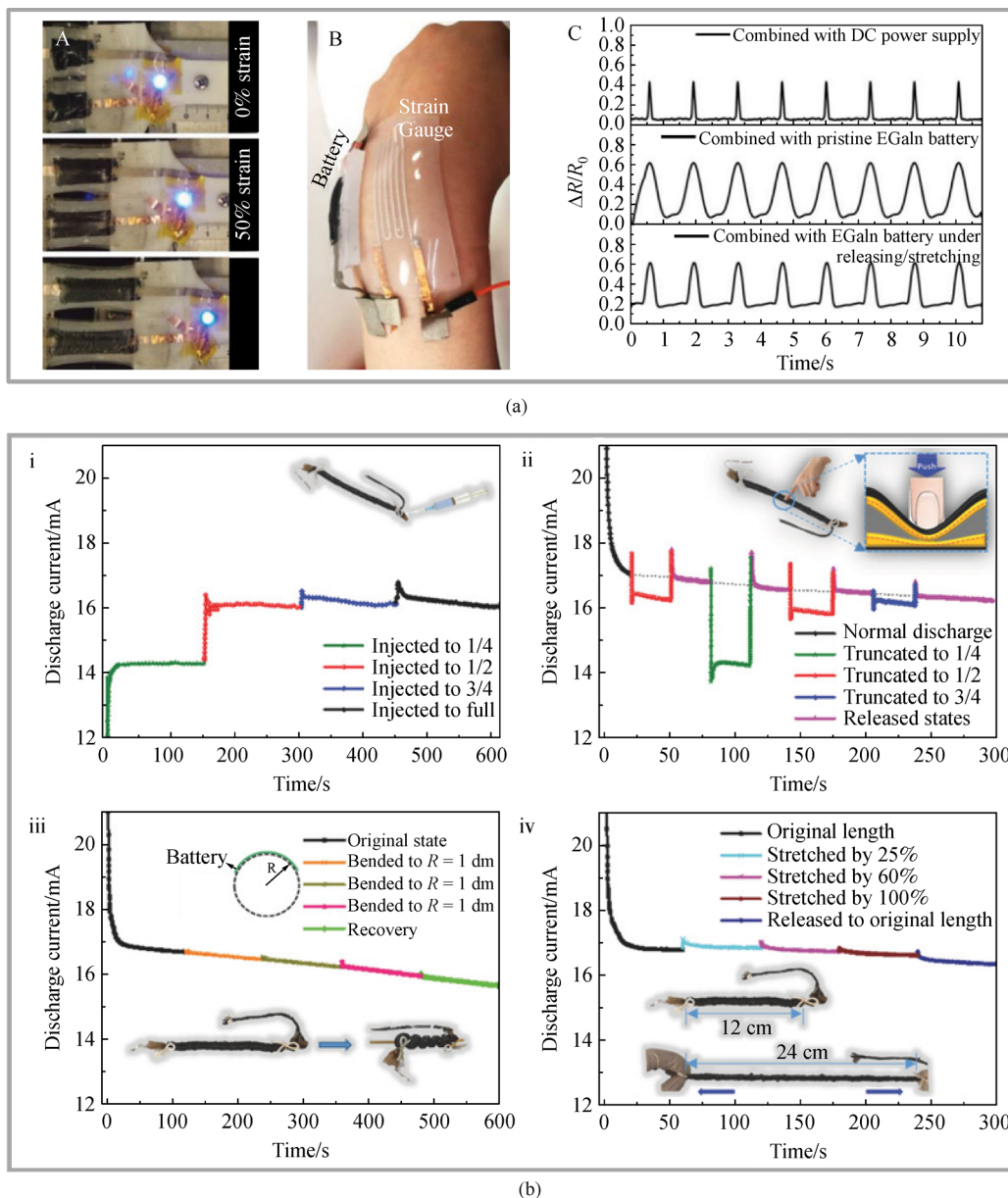


Fig. 7 Unique functionality of GBRTLMS based batteries.

(a) Flexibility and stretchability of sandwich-shaped GBRTLMS based batteries (i: photographs of the stretchable $\text{Ga}_{75}\text{In}_{25}\text{-MnO}_2$ battery array in series of two stretched under 0, 50, and 100% strain integrated with LEDs; ii: photograph of battery-powered strain sensor that is mounted on the wrist; iii: strain sensor measurements during stretching with a frequency of 1 Hz when powered with a DC power supply, pristine $\text{Ga}_{75}\text{In}_{25}\text{-MnO}_2$ battery, and releasing/stretching $\text{Ga}_{75}\text{In}_{25}\text{-MnO}_2$ battery, respectively (adapted with permission from Ref. [123]); (b) unique functions of electrochemical performance of the cable shaped $\text{GaIn}_{10}\text{-air}$ battery under different operations (i: injecting; ii: truncating; iii: bending; iv: stretching (adapted with permission from Ref. [120])).

demonstrated that the self-healing ability of Ga films was limited. As the cycle went on, the effective self-healing areas decreased gradually, and the reversible capacity of the battery reduced seriously. After 25 cycles, large-size cracks of $10\ \mu\text{m}$ appeared on the film electrode, and the reversible capacity declined to $245.7\ \text{mA}\cdot\text{h/g}$, with a capacity retention rate of only 44.2%. The decreased self-healing ability of Ga may be related to the formation of the

SEI film, which may attach to the crack surface and isolate Ga in different areas. To achieve a better self-healing ability, Ga-Sn liquid alloy was stabilized in a reduced graphene oxide (RGO)/ carbon nanotube (CNT) skeleton to be the anode for LIBs [5]. The RGO/CNT skeleton improved the electrical conductivity and prevented the GBRTLMS detaching from the current collector. The new anode ended up exhibiting an excellent cycle performance,

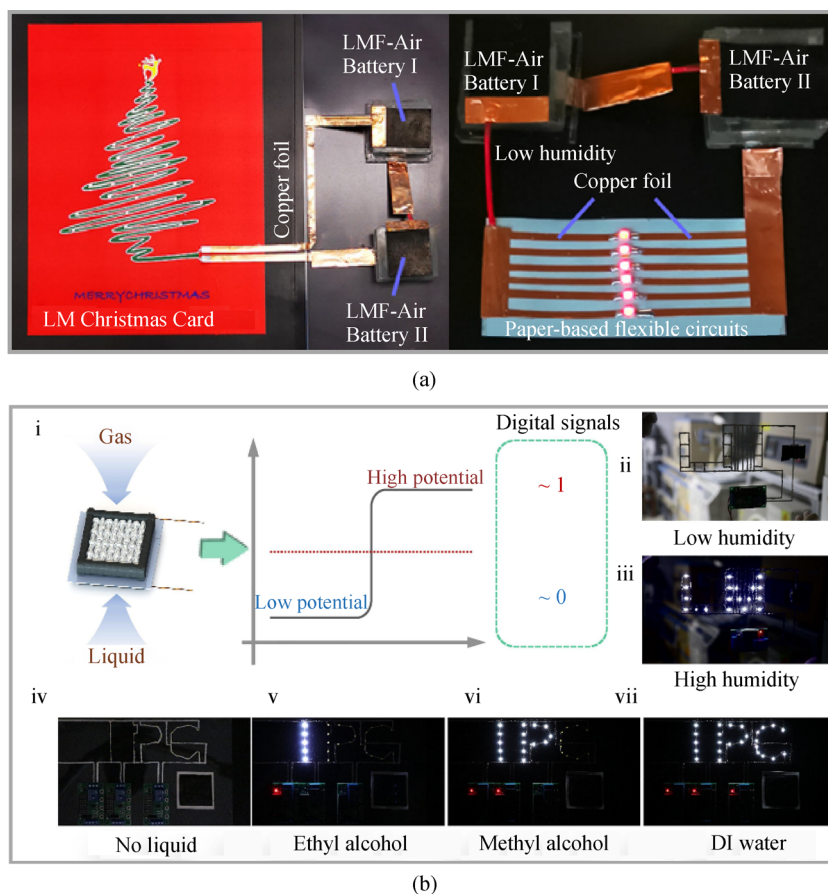


Fig. 8 Multi-functionality of batteries enabled by GBRTLMs.

(a) Applications of liquid metal foam-air battery in DIY cards and light-emitting diodes (adapted with permission from Ref. [121]); (b) illustration of signal conversion principle and two demonstration experiments for all-in-one liquid metal-air battery (adapted with permission from Ref. [51]).

retaining nearly a capacity of 100% within 4000 cycles. Moreover, researchers have confined GBRTLMs on Mxene paper carrier [144], interwoven carbon nanofiber [145], and porous carbon matrix [100] to avoid the influence of surface tension and fabricate freestanding electrodes.

3.2.2 Non-lithium batteries

GBRTLMs also play important roles in ameliorating the interfacial issues in non-lithium batteries, such as zinc-ion batteries (ZIBs) and aluminum-ion batteries (AIBs). Attributed to their high theoretical specific capacity ($820 \text{ mA} \cdot \text{h/g}$) and non-flammability in aqueous electrolytes, ZIBs are one of the promising alternatives for meeting the requirements of high energy density and safety [144–146]. Similar to lithium batteries, ZIBs are also faced with serious dendrite problems, accompanied with inevitable corrosion of zinc anode, which greatly affects the lifespan of ZIBs [147]. Through Ga-In-Zn phase diagrams, Liu et al. [146] designed an alloying liquid interlayer by coating liquid Ga-In alloy on Zn (GaIn@Zn) anode.

Through this process, a liquid-liquid interface (about $30 \mu\text{m}$ thick) was established to regulate the deposition behaviors of Zn anode. It was experimented that the charge capacity of GaIn@Zn anode can reach more than $12 \text{ mA} \cdot \text{h/cm}^2$ at 1 Ma/cm^2 , while that of bare Zn was less than $6 \text{ mA} \cdot \text{h/cm}^2$. Moreover, the Tafel curve suggested that the overpotential of the modified electrode was improved effectively and thus helped resist the corrosion in electrolyte. These results illustrated that the introduction of GBRTLMs not only accelerated the mass transport but also enhanced the long-term cycling stability of electrodes (Fig. 10(a)). The advantages of AIBs mainly lie in their low-cost, high-energy density, and safety [148]. Meanwhile, Al anodes are faced with critical problems, including dendrite, corrosion, and pulverization. Jiao et al. [149] introduced liquid Ga as the negative electrodes of Al batteries. When Al foil was used as the negative electrode of the battery, it corroded and pulverized after 28 cycles, while Ga maintained in liquid state after 100 cycles as illustrated in Fig. 10(b). But the unstable liquid-liquid interface between Ga and electrolyte determined that it was only suitable for stationary energy storage.

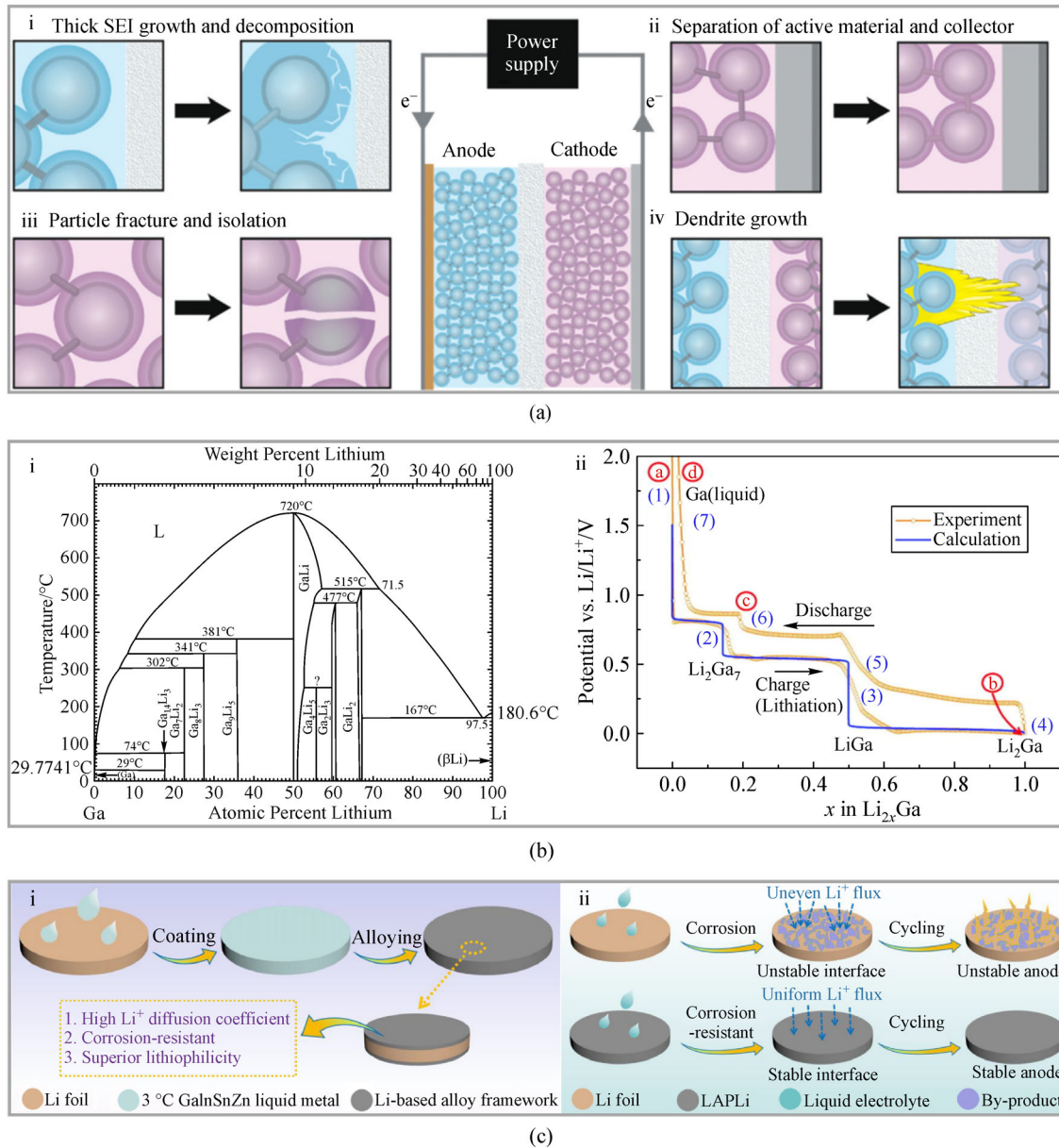


Fig. 9 Battery degradation mechanisms and GBRTLMs as functional additives in lithium batteries.

(a) Battery degradation mechanisms (i: formation and decomposition of unstable SEI; ii: separation of active material and current collector and loss of electrical conductivity; iii: particle cracking and subsequent isolation due to repeated Li-ion intercalation; iv: dendrite growth from anode causes short-circuits and potential thermal runaway (adapted with permission from Ref. [130]); (b) Ga-Li binary alloy system (i: Ga-Li phase diagram; ii: galvanostatic voltage-capacity profile of Ga at 40°C in the first cycle at C/50 (adapted with permission from Refs. [75,139]); (c) GBRTLM as anode in LMB (i: schematic showing the fabrication process of Li-based alloy passivated Li metal (LAPLi); ii: schematics showing the electrochemical behaviors of bare Li and LAPLi, respectively (adapted with permission from Ref. [137]).

3.3 Gallium-based liquid metals as interconnecting electrodes in multi-scenarios

In addition to electrochemical batteries, devices such as photovoltaics solar cells, generators, and SCs have also been widely exploited. Similarly, rigid and fragile materials have been phased out in order to meet the needs of deformable devices. Among them, connecting electrodes is a prerequisite for ensuring normal work under

deformation. In virtue of high stretchability and conductivity, GBRTLMs are born with the ability to be implemented as flexible and self-healable interconnecting electrodes.

3.3.1 Photovoltaics solar cells

Eutectic Ga-In liquid metal has been used in organic [12], organic-inorganic [159], perovskite [13] photovoltaics

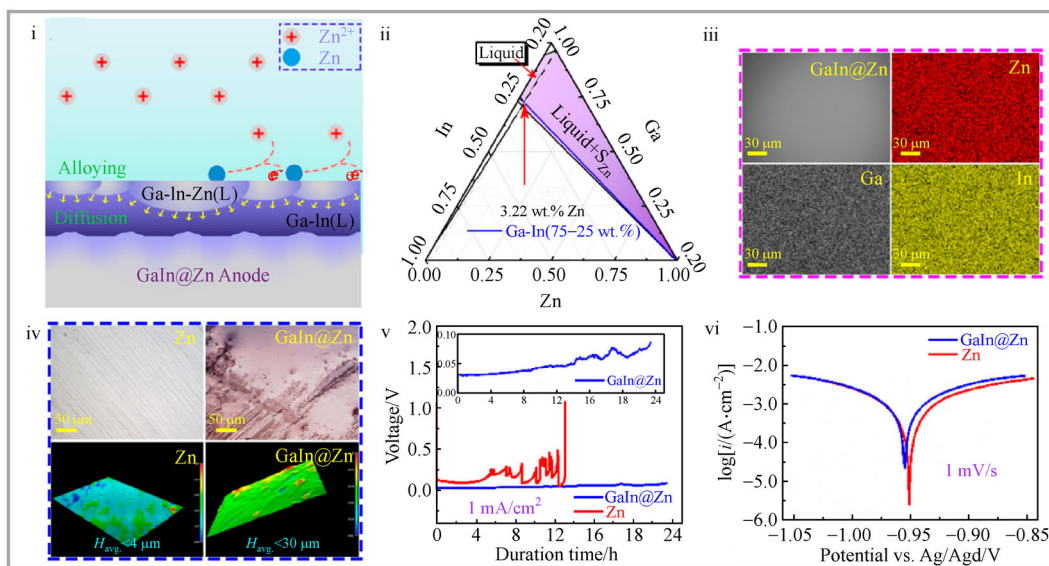
Table 4 GBRTLMS as auxiliary working electrodes in batteries

Year	Battery type	Liquid metal	Methods	Functionalities	Results	Ref.
2019	LMB	GaInSnZn	Coated on current collector	Reduced nucleation barrier	Improve coulombic efficiency; reduce voltage fluctuations	[135]
2020	LMB	Ga	Dropped onto Li	Self-repairing Li _x Ga layer	Long-term cycling life	[131]
2020	LMB	GaSn	Coated onto Li	Self-healing SEI layer	Superb rate capacity; long-term cycling life	[134]
2020	LMB	GaInSnZn	Coated on Mxene	Amorphous nucleation seeds	Improve coulombic efficiency	[136]
2021	LMB	GaInSnZn	Formed alloy with Li	Passivate Li metal surface	Superior electrochemical performance	[137]
2008	LIB	Ga	Confined in a carbon matrix	Self-healing	Buffer volume change	[100]
2011	LIB	Ga	Applied onto stainless steel	Self-healing	Higher capacity and higher durability of electrode	[75]
2015	LIB	Ga film	Applied onto stainless steel	Self-healing	Capacity decreased gradually	[101]
2017	LIB	Ga ₈₈ Sn ₁₂	Supported by carbon skeleton	Self-healing	Improve cycle life; deliver high capacity	[5]
2018	LIB	Galinstan	Embedded in N-rGO with Si	Heal the crack	High coulombic efficiency; better mechanical behavior	[150]
2018	LIB	Ga ₇₀ In ₂₀ Sn ₁₀	Coated on Cu foil with Si	Spontaneous repairing	High capacity and stability; high coulombic efficiency	[143]
2018	LIB	Ga _{12.6} Sn _{1.0}	Composited with Si	Self-healing; liquid buffer	High capacity; excellent cyclic performance	[151]
2018	LIB	Ga	Encapsulated by interwoven carbon fibers	Prevent the agglomeration	High capacity; high cycling stability; good rate performance	[152]
2019	LIB	Ga	Coated on Cu film	Self-healing	High capacity; better rate performance	[153]
2019	LIB	Ga ₈₈ Sn ₁₂	Coated with a carbon shell	Self-healing	Excellent capacity; stable cycling performance	[154]
2019	LIB	GaInSnZn	Confined in Mxene paper	Conductive substrate	Flexible and binder-free anode; high capacity and cycling	[155]
2020	LIB	Ga ₉₂ Sn ₈	Paired with polymer	Self-healing	Maintain mechanical integrity and better contact	[156]
2020	LIB	Galinstan	Introduced between Si/Cu	Self-healing	Avoid interfacial delamination; avoid early capacity decay	[157]
2021	LIB	Ga	In situ form	Self-healing	Improve the cycling stability	[158]
2021	ZIB	GaIn	Coating on zinc anode	Inward deposition	Ameliorate dendrite growth and electrode corrosion	[146]
2020	ALIB	Ga	Replace Al	Self-healing	Dendrite-free; corrosion-resistant; non-pulverization	[149]

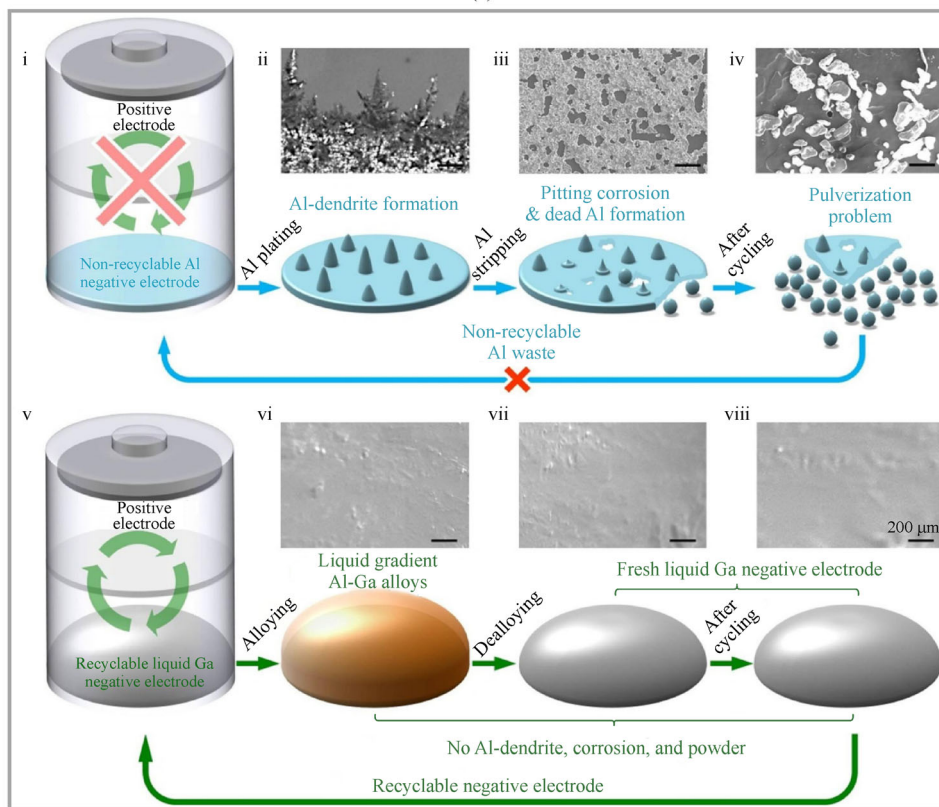
Notes: N-rGO (N-doped reduced graphene oxide).

solar cells, which allows high mechanical stability of the device without any degradation of performance over repeated bending. In organic solar cells, organic semiconductors have a relatively low charge mobility, thus an electrical contact to the cell must cover the active surface without shorting the device and provide uniform contact to the organic film [160]. Aluminum, having a work function of 4.3 eV, is most widely used in organic cells as a top metal contact through the method of costly, time-consuming vacuum thermal metal evaporation. The work function of GaIn₂₅ is very close to Al. Besides, it is non-toxic and in liquid state at room temperature, which greatly facilitates the process of depositing under an environmental condi-

tion [161]. This offers a simple vacuum-free and inexpensive method compared with the Al electrodes, making GaIn₂₅ a good candidate for replacing the Al as illustrated in Fig. 11(a). GaIn₂₅ has gradually been used as top contact in the field of testing the photovoltaic characteristics of organic solar cells [11,12,160–163]. Core-shell-structured Ga-In-Sn-Zn eutectic alloy microcapsules were used as self-healing conductors for sustainable and flexible perovskite solar cells [13]. Pressing or cutting causes the capsule to break, and liquid metal inside can flow out to repair the damaged parts of the wire (Fig. 11(b)). The results exhibited a power conversion efficiency retention (PCE) of 99% relative to the initial



(a)



(b)

Fig. 10 GBRTLMS as auxiliary working electrodes in non-lithium batteries.

(a) GaIn interlayer for aqueous ZIB (i: schematic illustration of alloying-diffusion synergistic dendrite-free GaIn@Zn anode surface evolution; ii: Ga-In-Zn ternary isothermal section phase diagram at 25°C; iii: surface SEM images and elemental maps of GaIn@Zn anode; iv: surface optical microscopy images and 3D simulation height of Zn and GaIn@Zn anode; v: overcharging test of Zn and GaIn@Zn symmetric cells at 1 mA/cm²; vi: tafel curves of Zn and GaIn@Zn anode under three-electrode system: graphite rod (CE), Zn or GaIn@Zn anode (WE), or Ag/AgCl (RE) (adapted with permission from Ref. [146])); (b) Ga as negative electrode for Al-ion batteries (i: sketch of the evolutionary mechanism of several critical problems (dendrite, corrosion, pulverization, and non-recyclable Al waste) of Al foil negative electrode; ii–iv: SEM images of pristine, after electroplating, after 28 cycles, and after 100 cycles of Al foil negative electrode; v: sketch of the evolutionary process of the novel dendrite-free, corrosion resistant, non-pulverization and recyclable liquid Ga negative electrode; vi–viii: SEM images of pristine, after electrochemical alloying, after electrochemical dealloying, and after 1000 cycles of Ga negative electrode (adapted with permission from Ref. [149]).

value. An intrinsic mechanically recoverable organic-inorganic perovskite solar cell utilizing Ga-In alloy as stretchable electrodes was presented in Fig. 11(c). It successfully prevented mechanical damage of the perovskite layer during bending and crumpling. After recovery from crumpling, the PCE of the device dropped to 6.1% from the initial value of 10.2% [159]. The development of self-healing and shape-recoverable solar cells is expected to provide a wearable energy source for practical applications.

3.3.2 Generators

GBRTLMS have been exploited in a series of electrical generators. The present laboratory had ever [43,164] proposed different liquid metal based magnetohydrodynamics generators to harvest human energy and power for wearable micro/nano devices. Such strategy also works for harvesting waste heat to power thermoelectric generator [165]. Recently, all kinds of flexible nanogenerators enabled by soft GBRTLMS electrodes have been further studied, including triboelectric nanogenerators (TENGs) [8,166,167], thermoelectric nanogenerators (TEGs) [7,168,169], and piezoelectric nanogenerators (PENGs) [170,171].

TENGs, based on the coupling of the triboelectric effect and the electrostatic induction phenomenon, have four basic operating modes, including the vertical contact-separation mode, the lateral sliding mode, the single-electrode mode, and the freestanding triboelectric-layer mode [172]. Conventional TENGs mainly uses solid electrode materials such as Al and Cu. Therefore, the contact efficiency is greatly affected by the roughness between the two layers [173]. Tang et al. [167] developed a GBRTLMs-based TENG as shown in Fig. 12(a). It had a contact area of 15 cm² and could generate a voltage of 679 V and a current of 9 μ A. Moreover, compared with solid-solid contact TENGs, it can achieve over four times more output charge density (430 $^{\circ}$ C/m²) and higher energy conversion efficiency (70.6%). Intrinsically stretchable and self-healable GBRTLMS not only guarantee a total electrical contact, but also maintain a low resistance even under large deformation and multiple freedom degrees. Using the silicone rubber layer as a triboelectric and encapsulation material, a GBRTLM-electrode-based stretchable TENG was designed to harvest energy from irregular and low-frequency human motions through a patch or integrated into clothing to drive wearable electronic devices [174]. GBRTLMS can also give TENGs more features. They can act as phase change materials with melting points in the comfortable temperature range of human skin, realizing a self-powered thermoregulating electronic skin (TE-skin) (Fig. 12(b)) [166].

Just like TENGs, GBRTLMS have been explored to

achieve a complete contact in soft PENGs [171] and TEGs [7,44,169]. It is worth mentioning that in TEGs, GBRTLMS is generally composited with elastomers. GBRTLMS can be effective additives to transform elastomers into multifunctional composites [19,170]. The most common method is to enclose GBRTLMS in an elastomer, or dope with other functional materials like graphene nanoplatelets at the same time. Zadan et al. [169] proposed a soft and stretchable TEGs utilizing GBRTLMS embedded elastomer as material interface. The elastomer contained a mechanically sintered pattern to provide electrical connections between p-type and n-type Bi₂Te₃ semiconductors. Owing to the ductility of liquid metal and elastomer, they did not electrically or mechanically fail when stretched to strain above 50% (Fig. 12(c)). Moreover, flexible connection provides a pathway for the realization of seamless integration. PENG and TENG were reasonably integrated by Yang et al. [8]. A stretchable piezoelectric-enhanced TENG was fabricated to achieve a higher output performance as illustrated in Fig. 12(d).

3.3.3 SCs

SCs, known as electrochemical capacitors, are different from typical batteries in materials, structures, and charge storage mechanisms. Typical batteries storage charge in bulk electrodes while SCs via surface. The different mechanisms determine their different characteristics [175]. SCs have noteworthy priorities such as long cycle life, simple structure, and fast rates of charge and discharge [9]. Traditional SCs are made of hard and brittle materials, which are ubiquitous for electrodes and connectors. The development of flexible integrated device microsystem poses new challenges to SCs. They should not lose performance or even fail in multiple mechanical deformations [10]. GBRTLMS could be potential candidates as soft electrode materials for flexible SCs because of their insulating surface oxide layer for electric double layer formation [176]. Kim et al. [10] used Ga-In alloy integrated with oxygen functionalized CNTs as electrodes to construct all-soft SCs for soft microsystems (Fig. 13(a)). The constructed SCs exhibited an area capacitance of 12.4 mF/cm² which remained nearly unchanged under an applied strain of 30%. With the increased investigation into the integrated flexible and foldable SCs [177–179], the mechanically stable interconnections between the devices have also become more intractable. Special structures like serpentine are designed to solve the connection problem, which often require complicated processing [180]. Maintaining a superior conductivity and conformability even under high deformability, GBRTLMS are proper alternatives for flexible electrical connections which can achieve desired functions through simple fabricate processes [32]. With GBRTLMS patterned as interconnections on paper as substrate, a foldable and deformable sensor

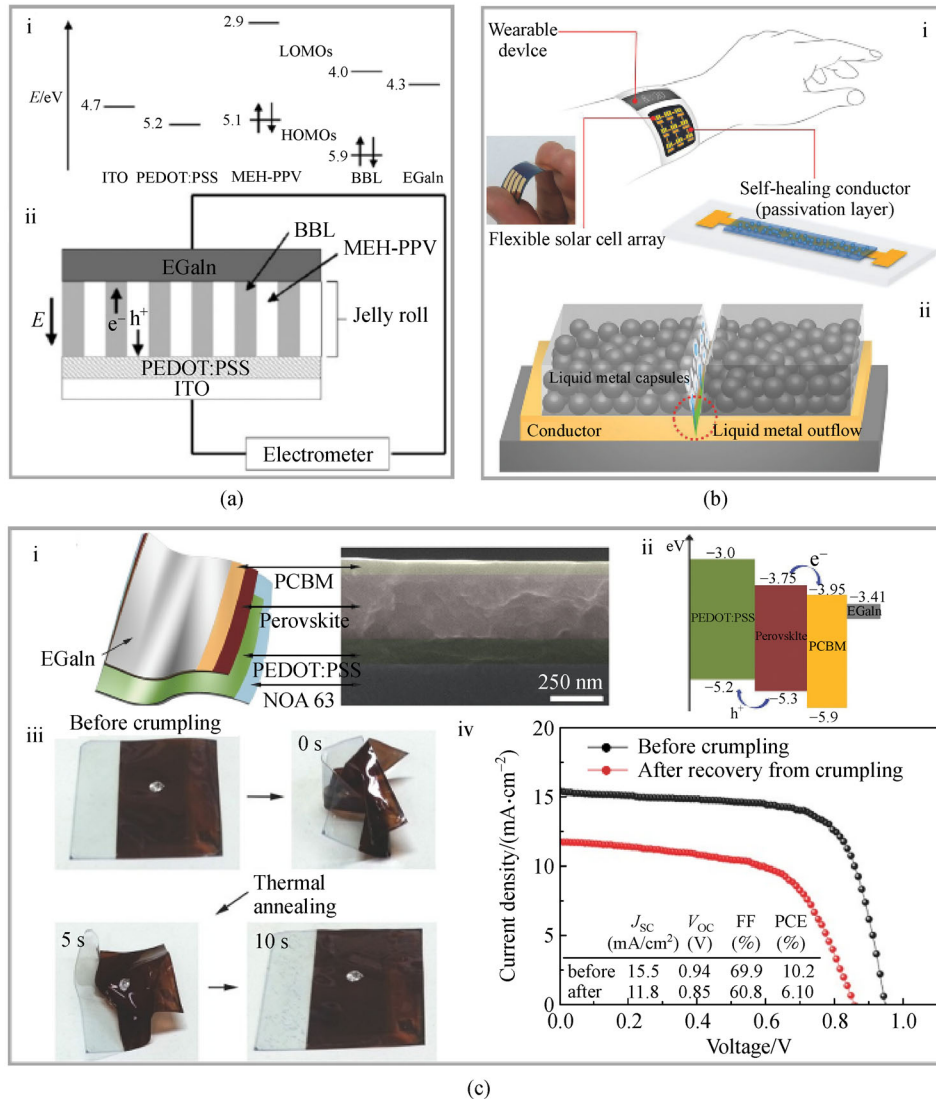


Fig. 11 GBRTLs as electrodes in photovoltaic solar cells.

(a) Schematic of GaIn₂₅ used as top contact in the field of solar cells (i: energy level diagram showing the vacuum-level position of work functions; ii: the junction used to measure a photovoltaic response of a jelly roll (adapted with permission from Ref. [11]); (b) liquid metal microcapsules as self-healing conductors in solar cells (i: schematic of solar-powered smart watch with self-healing conductors; ii: schematic illustrating the healing mechanism of a metal conductor: liquid metal flows out from the ruptured microcapsules and is transported to the damaged site (adapted with permission from Ref. [13]); (c) device architecture of ultraflexible and shape recoverable perovskite solar cell (i: schematic of the stacked layers and a cross-sectional SEM image of the device; ii: schematic of an energy diagram; iii: photographs showing the state of device during the crumpling test and thermal annealing was achieved by placing the crumpled device on a hot plate at 80°C for 10 s; iv: current density-voltage ($J-V$) curves measured before and after shape recovery from crumpling test (adapted with permission from Ref. [159]).

system was constructed driven by integrated micro-SCs (Fig. 13(b)) [9]. The system showed a mechanically stable ultraviolet (UV) light sensing even under repetitive folding cycles.

4 Summary and perspective

In summary, GBRTLs are intrinsically excellent combinations of liquidity, metallicity, and biocompatibility. The metallicity is the premise for their applications as

electrodes. The liquidity is the guarantee of the fast kinetics and the self-healing characteristic. The biocompatibility ensures their extensive use in daily life. In these regards, GBRTLs demonstrate potentials to be battery materials in the field of portable devices and epidermal electronics. Nevertheless, it is worth noting that some issues must be taken into consideration. First, their prices are not competitive, which determine that they are not suitable for large-scale energy storage. Then, corrosion may occur when GBRTLs are in contact with Al and Cu. Thus, the construction materials of the batteries need to be

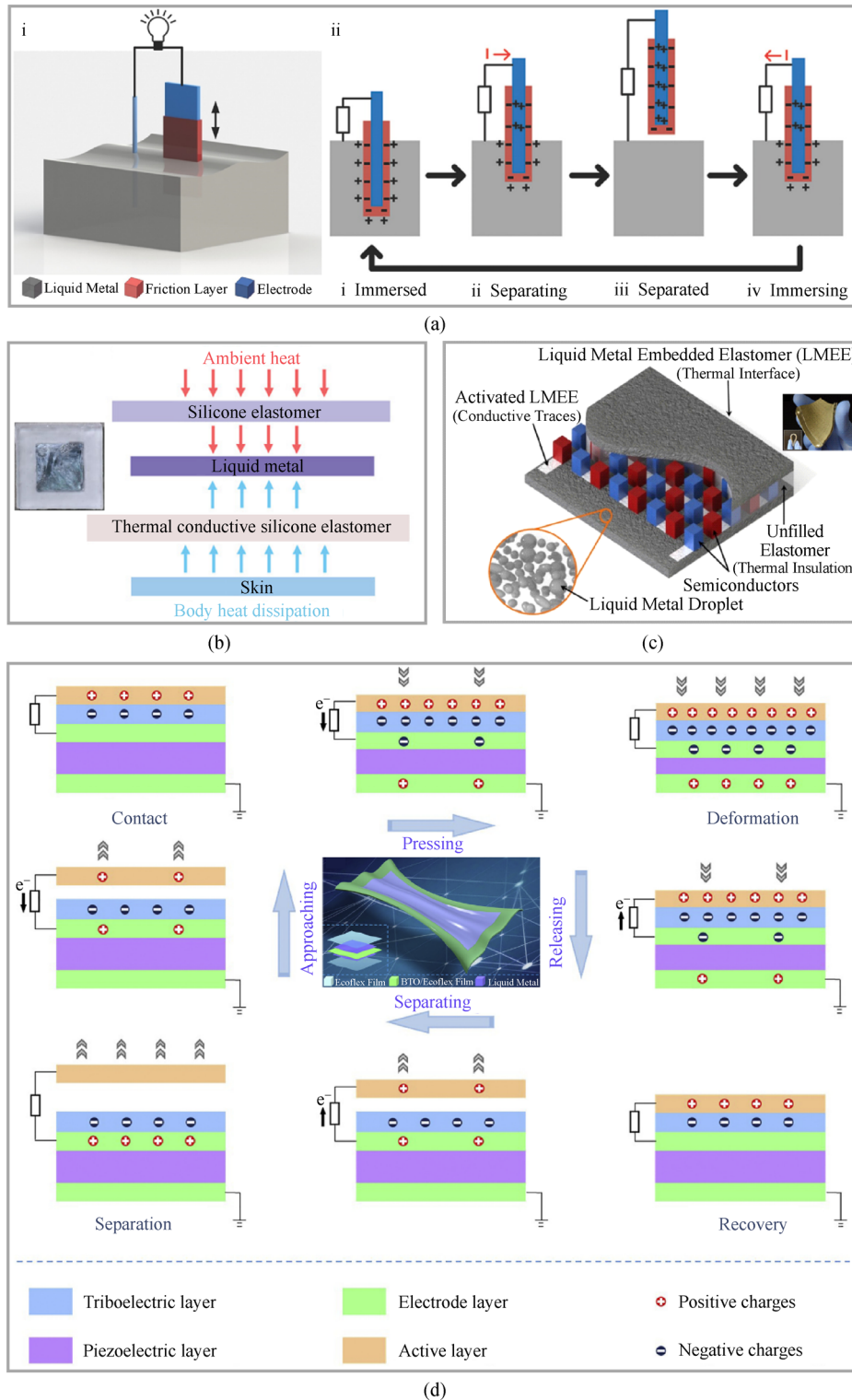


Fig. 12 GBRTLMs as electrodes in generators.

(a) Working principle of the liquid-metal-based TENG (LM-TENG) (i: the device configuration of LM-TENG; ii: step-by step illustration of the working principle of LM-TENG (adapted with permission from Ref. [167]); (b) schematic diagram of GBRTLMs based dynamic self-powered TE-skin (inset: photograph of the TE-skin with a scale bar of 1 cm) (adapted with permission from Ref. [166]); (c) stretchable TEG with liquid metal embedded elastomer composites as the material interface on the top and bottom to provide connections between p-type and n-type Bi_2Te_3 semiconductors (inset: photos of fabricated TEG under deformation and complete bend) (adapted with permission from Ref. [169]); (d) the working principle of liquid metal electrode based stretchable piezoelectric-enhanced TENG (adapted with permission from Ref. [8]).

screened. Besides, the high surface tension of GBRTLMs may cause poor contact among current collector, electrodes, and electrolyte. Therefore, extra special treatment is required for GBRTLMs to realize a better wetting.

As the main reacting electrodes, GBRTLMs have given the battery unique functions such as flexibility, wearability, and printability. Moreover, the batteries are promising as deformable energy storage devices in harsh environments at low temperatures. However, most of the flexible GBRTLMs-based batteries reported now are primary batteries. Novel electrode materials which may have a

higher theoretical capacity and energy density still need to be identified.

In terms of the auxiliary functional electrodes, the self-healing property of GBRTLMs have significantly extended the performance and lifespan of batteries. Nevertheless, the performance of GBRTLMs self-healing electrodes is still not completely satisfactory, especially in the aspect of capacity. In addition, the self-healing mechanism of liquid Ga has not been clearly studied.

For interconnecting electrodes, GBRTLMs have been applied in multi-scenarios, making flexible integrated

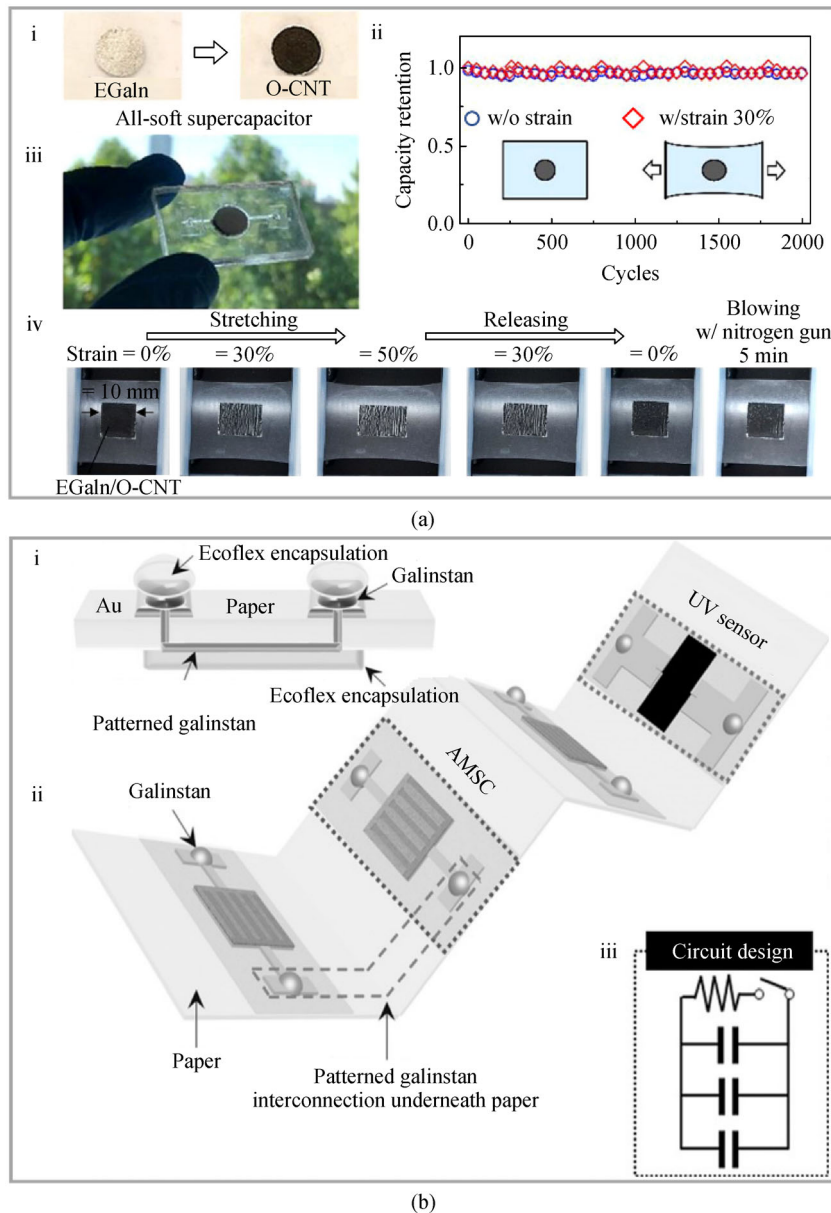


Fig. 13 GBRTLMs as electrodes in SCs.

(a) All soft SCs based on functionalized oxygen CNTs eutectic gallium-indium liquid metal (O-CNT/EGaIn) electrodes (i: functionalized EGaIn electrode; ii: capacity retention subject to charging/discharging cycles for SCs with/without applied strain of 30%; iii: photo of all-soft SCs; iv: mechanical stability of O-CNT/EGaIn electrode under stretching deformation up to 50% and subject to nitrogen flow for 5 min (adapted with permission from Ref. [10]); (b) a UV sensor driven by asymmetric micro-SCs (AMSCs) on a liquid metal patterned foldable paper (i: cross-section view of the integrated AMSCs with Galinstan interconnections; ii: schematic illustration; iii: circuit design (adapted with permission from Ref. [9])).

systems possible. Soft batteries can be flawlessly incorporated into sensing systems without cumbersome external battery power, thus meeting the micro and light needs of wearable devices.

At present, most of the reported GBRTLMs based batteries are still in the prototype stage. There is still a long way to go before these batteries can be commercialized on epidermal electronic occasions. This depends on the cross-application and integration of interdisciplinary knowledge, including electrochemistry, flexible electronics, sensing, materials science, and so on.

Acknowledgements This work was supported by the National Natural Science Foundation of China (Grant No. 91748206), and the National Key Research and Development Program of China (No. 2020YFC0122301).

References

- Jia D, Liu J. Human power-based energy harvesting strategies for mobile electronic devices. *Frontiers of Energy and Power Engineering in China*, 2009, 3(1): 27–46
- Cairns E J, Shimotake H. High-temperature batteries. *Science*, 1969, 164(3886): 1347–1355
- Liu Y, Wang W, Ghadimi N. Electricity load forecasting by an improved forecast engine for building level consumers. *Energy*, 2017, 139: 18–30
- Akbary P, Ghiasi M, Pourkheranjani M R R, et al. Extracting appropriate nodal marginal prices for all types of committed reserve. *Computational Economics*, 2019, 53(1): 1–26
- Wu Y, Huang L, Huang X, et al. A room-temperature liquid metal-based self-healing anode for lithium-ion batteries with an ultra-long cycle life. *Energy & Environmental Science*, 2017, 10(8): 1854–1861
- Krupenkin T, Taylor J A. Reverse electrowetting as a new approach to high-power energy harvesting. *Nature Communications*, 2011, 2(1): 448
- Zhu P, Shi C, Wang Y, et al. Recyclable, healable, and stretchable high-power thermoelectric generator. *Advanced Energy Materials*, 2021, 11(25): 2100920
- Yang C, He J, Guo Y, et al. Highly conductive liquid metal electrode based stretchable piezoelectric-enhanced triboelectric nanogenerator for harvesting irregular mechanical energy. *Materials & Design*, 2021, 201: 109508
- Yun J, Lim Y, Lee H, et al. A patterned graphene/ZnO UV sensor driven by integrated asymmetric micro-supercapacitors on a liquid metal patterned foldable paper. *Advanced Functional Materials*, 2017, 27(30): 1700135
- Kim M G, Lee B, Li M, et al. All-soft supercapacitors based on liquid metal electrodes with integrated functionalized carbon nanotubes. *ACS Nano*, 2020, 14(5): 5659–5667
- Lipomi D J, Chiechi R C, Reus W F, et al. Laterally ordered bulk heterojunction of conjugated polymers: nanoskiving a jelly roll. *Advanced Functional Materials*, 2008, 18(21): 3469–3477
- Lipomi D J, Tee B C K, Vosgueritchian M, et al. Stretchable organic solar cells. *Advanced Materials*, 2011, 23(15): 1771–1775
- Chu K, Song B G, Yang H I, et al. Smart passivation materials with a liquid metal microcapsule as self-healing conductors for sustainable and flexible perovskite solar cells. *Advanced Functional Materials*, 2018, 28(22): 1800110
- Song Z, Ma T, Tang R, et al. Origami lithium-ion batteries. *Nature Communications*, 2014, 5(1): 3140
- Song Z, Wang X, Lv C, et al. Kirigami-based stretchable lithium-ion batteries. *Scientific Reports*, 2015, 5(1): 10988
- Wang Y, Chen C, Xie H, et al. 3D-printed all-fiber Li-ion battery toward wearable energy storage. *Advanced Functional Materials*, 2017, 27(43): 1703140
- Xu S, Zhang Y, Cho J, et al. Stretchable batteries with self-similar serpentine interconnects and integrated wireless recharging systems. *Nature Communications*, 2013, 4(1): 1543
- Silva C A, Lv J, Yin L, et al. Liquid metal based island-bridge architectures for all printed stretchable electrochemical devices. *Advanced Functional Materials*, 2020, 30(30): 2002041
- Chen S, Wang H, Zhao R, et al. Liquid metal composites. *Matter*, 2020, 2(6): 1446–1480
- Daeneke T, Khoshmanesh K, Mahmood N, et al. Liquid metals: fundamentals and applications in chemistry. *Chemical Society Reviews*, 2018, 47(11): 4073–4111
- Ge H, Li H, Mei S, et al. Low melting point liquid metal as a new class of phase change material: an emerging frontier in energy area. *Renewable & Sustainable Energy Reviews*, 2013, 21: 331–346
- Li H, Liu J. Revolutionizing heat transport enhancement with liquid metals: proposal of a new industry of water-free heat exchangers. *Frontiers in Energy*, 2011, 5(1): 20–42
- Zhang X, Li X, Zhou Y, et al. Vascularized liquid metal cooling for thermal management of kW high power laser diode array. *Applied Thermal Engineering*, 2019, 162: 114212
- Gao J, Zhang X, Fu J, et al. Numerical investigation on integrated thermal management via liquid convection and phase change in packed bed of spherical low melting point metal macrocapsules. *International Journal of Heat and Mass Transfer*, 2020, 150: 119366
- Ma K, Liu J. Liquid metal cooling in thermal management of computer chips. *Frontiers of Energy and Power Engineering in China*, 2007, 1(4): 384–402
- Ma K, Liu J. Nano liquid-metal fluid as ultimate coolant. *Physics Letters A*, 2007, 361(3): 252–256
- Yang X, Liu J. Liquid metal enabled combinatorial heat transfer science: toward unconventional extreme cooling. *Frontiers in Energy*, 2018, 12(2): 259–275
- Liu G, Liu J. Convective cooling of compact electronic devices via liquid metals with low melting points. *Journal of Heat Transfer*, 2021, 143(5): 050801
- Fu J, Gao J, Chen S, et al. Self-encapsulation liquid metal materials for flexible and stretchable electrical conductors. *RSC Advances*, 2019, 9(60): 35102–35108
- Guo R, Wang H, Sun X, et al. Semiliquid metal enabled highly conductive wearable electronics for smart fabrics. *ACS Applied Materials & Interfaces*, 2019, 11(33): 30019–30027
- Qin P, Wang L, Liu T, et al. The design and manufacturing process of an electrolyte-free liquid metal frequency-reconfigurable antenna. *Sensors (Basel)*, 2021, 21(5): 1793

32. Yang J, Cheng W, Kalantar-Zadeh K. Electronic skins based on liquid metals. *Proceedings of the IEEE*, 2019, 107(10): 2168–2184
33. Tian L, Gao M, Gui L. A microfluidic chip for liquid metal droplet generation and sorting. *Micromachines*, 2017, 8(2): 39
34. Ye Z, Zhang R, Gao M, et al. Development of a high flow rate 3-D electroosmotic flow pump. *Micromachines*, 2019, 10(2): 112
35. Zhang R, Ye Z, Gao M, et al. Liquid metal electrode-enabled flexible microdroplet sensor. *Lab on a Chip*, 2020, 20(3): 496–504
36. Khoshmanesh K, Tang S, Zhu J, et al. Liquid metal enabled microfluidics. *Lab on a Chip*, 2017, 17(6): 974–993
37. Yuan B, Zhao C, Sun X, et al. Liquid-metal-enhanced wire mesh as a stiffness variable material for making soft robotics. *Advanced Engineering Materials*, 2019, 21(10): 1900530
38. Liu T, Qin P, Liu J. Intelligent liquid integrated functional entity: a basic way to innovate future advanced biomimetic soft robotics. *Advanced Intelligent Systems*, 2019, 1(3): 1970030
39. Yao Y, Liu J. Liquid metal wheeled small vehicle for cargo delivery. *RSC Advances*, 2016, 6(61): 56482–56488
40. Hou Y, Sun Z, Rao W, et al. Nanoparticle-mediated cryosurgery for tumor therapy. *Nanomedicine; Nanotechnology, Biology, and Medicine*, 2018, 14(2): 493–506
41. Yi L, Jin C, Wang L, et al. Liquid-solid phase transition alloy as reversible and rapid molding bone cement. *Biomaterials*, 2014, 35(37): 9789–9801
42. Sun X, Sun M, Liu M, et al. Shape tunable gallium nanorods mediated tumor enhanced ablation through near-infrared photothermal therapy. *Nanoscale*, 2019, 11(6): 2655–2667
43. Jia D, Liu J, Zhou Y. Harvesting human kinematical energy based on liquid metal magnetohydrodynamics. *Physics Letters A*, 2009, 373(15): 1305–1309
44. Li H, Zhou Y, Liu J. Liquid metal based printable thermoelectric generator and its performance evaluation. *Scientia Sinica: Technologica*, 2014, 44(4): 407–416 (in Chinese)
45. Xu S, Liu J. Metal-based direct hydrogen generation as unconventional high density energy. *Frontiers in Energy*, 2019, 13(1): 27–53
46. Yi L, Ding Y, Yuan B, et al. Breathing to harvest energy as a mechanism towards making a liquid metal beating heart. *RSC Advances*, 2016, 6(97): 94692–94698
47. Tang J, Wang J, Liu J, et al. A volatile fluid assisted thermo-pneumatic liquid metal energy harvester. *Applied Physics Letters*, 2016, 108(2): 023903
48. Zhang Q, Liu J. Nano liquid metal as an emerging functional material in energy management, conversion and storage. *Nano Energy*, 2013, 2(5): 863–872
49. Ge H, Liu J. Phase change effect of low melting point metal for an automatic cooling of USB flash memory. *Frontiers in Energy*, 2012, 6(3): 207–209
50. Jahn D, Plust H G. Possible use of gallium as negative electrode in galvanic cells. *Nature*, 1963, 199(4895): 806–807
51. Wang Y, Wang X, Xue M, et al. All-in-one ENERGISER design: smart liquid metal-air battery. *Chemical Engineering Journal*, 2021, 409: 128160
52. Park S, Thangavel G, Parida K, et al. A stretchable and self-healing energy storage device based on mechanically and electrically restorative liquid-metal particles and carboxylated polyurethane composites. *Advanced Materials*, 2019, 31(1): 1805536
53. Guo X, Ding Y, Yu G. Design principles and applications of next-generation high-energy-density batteries based on liquid metals. *Advanced Materials*, 2021, 33(29): 2100052
54. Li Q, He G, Ding Y. Applications of low-melting-point metals in rechargeable metal batteries. *Chemistry (Weinheim an der Bergstrasse, Germany)*, 2021, 27(21): 6407–6421
55. Zhang S, Liu Y, Fan Q, et al. Liquid metal batteries for future energy storage. *Energy & Environmental Science*, 2021, 14(8): 4177–4202
56. Mirzapour F, Lakzaei M, Varamini G, et al. A new prediction model of battery and wind-solar output in hybrid power system. *Journal of Ambient Intelligence and Humanized Computing*, 2019, 10(1): 77–87
57. Leng H, Li X, Zhu J, et al. A new wind power prediction method based on ridgelet transforms, hybrid feature selection and closed-loop forecasting. *Advanced Engineering Informatics*, 2018, 36: 20–30
58. Hamian M, Darvishan A, Hosseinzadeh M, et al. A framework to expedite joint energy-reserve payment cost minimization using a custom-designed method based on Mixed Integer Genetic Algorithm. *Engineering Applications of Artificial Intelligence*, 2018, 72: 203–212
59. Kim H, Boysen D A, Newhouse J M, et al. Liquid metal batteries: past, present, and future. *Chemical Reviews*, 2013, 113(3): 2075–2099
60. Bradwell D J, Kim H, Sirk A H, et al. Magnesium-antimony liquid metal battery for stationary energy storage. *Journal of the American Chemical Society*, 2012, 134(4): 1895–1897
61. Wang K, Jiang K, Chung B, et al. Lithium–antimony–lead liquid metal battery for grid-level energy storage. *Nature*, 2014, 514(7522): 348–350
62. Ning X, Phadke S, Chung B, et al. Self-healing Li-Bi liquid metal battery for grid-scale energy storage. *Journal of Power Sources*, 2015, 275: 370–376
63. Li H, Wang K, Cheng S, et al. High performance liquid metal battery with environmentally friendly antimony-tin positive electrode. *ACS Applied Materials & Interfaces*, 2016, 8(20): 12830–12835
64. Li H, Yin H, Wang K, et al. Liquid metal electrodes for energy storage batteries. *Advanced Energy Materials*, 2016, 6(14): 1600483
65. Li H, Wang K, Zhou H, et al. Tellurium-tin based electrodes enabling liquid metal batteries for high specific energy storage applications. *Energy Storage Materials*, 2018, 14: 267–271
66. Weber N, Landgraf S, Mushtaq K, et al. Modeling discontinuous potential distributions using the finite volume method, and application to liquid metal batteries. *Electrochimica Acta*, 2019, 318: 857–864
67. Guo X, Ding Y, Gao H, et al. A ternary hybrid-cation room-temperature liquid metal battery and interfacial selection mechanism study. *Advanced Materials*, 2020, 32(22): 2000316
68. Zhou C, Li T. Research on liquid metal energy storage battery equalization management system in power PSS. *Procedia CIRP*, 2019, 83: 547–551
69. Aghajani G, Ghadimi N. Multi-objective energy management in a

- micro-grid. *Energy Reports*, 2018, 4: 218–225
70. Jin Y, Liu K, Lang J, et al. An intermediate temperature garnet-type solid electrolyte-based molten lithium battery for grid energy storage. *Nature Energy*, 2018, 3(9): 732–738
 71. Ding Y, Guo X, Qian Y, et al. Low-temperature multielement fusible alloy-based molten sodium batteries for grid-scale energy storage. *ACS Central Science*, 2020, 6(12): 2287–2293
 72. Lalau C C, Dimitrova A, Himmerlich M, et al. An electrochemical and photoelectron spectroscopy study of a low temperature liquid metal battery based on an ionic liquid electrolyte. *Journal of the Electrochemical Society*, 2016, 163(10): A2488–A2493
 73. Weber N, Galindo V, Stefani F, et al. Current-driven flow instabilities in large-scale liquid metal batteries, and how to tame them. *Journal of Power Sources*, 2014, 265: 166–173
 74. Weier T, Bund A, El-Mofid W, et al. Liquid metal batteries-materials selection and fluid dynamics. *IOP Conference Series. Materials Science and Engineering*, 2017, 228: 012013
 75. Deshpande R D, Li J, Cheng Y T, et al. Liquid metal alloys as self-healing negative electrodes for lithium ion batteries. *Journal of the Electrochemical Society*, 2011, 158(8): A845
 76. Ding Y, Guo X, Qian Y, et al. Room-temperature all-liquid-metal batteries based on fusible alloys with regulated interfacial chemistry and wetting. *Advanced Materials*, 2020, 32(30): 2002577
 77. Haxel G B, Hedrick J B, Orris G J. Rare earth elements: critical resources for high technology. *US Geological Survey Fact Sheet*, 2002, 087–02
 78. Yu S, Kaviani M. Electrical, thermal, and species transport properties of liquid eutectic Ga-In and Ga-In-Sn from first principles. *Journal of Chemical Physics*, 2014, 140(6): 064303
 79. Fu J, Zhang C, Liu T, et al. Room temperature liquid metal: its melting point, dominating mechanism and applications. *Frontiers in Energy*, 2020, 14(1): 81–104
 80. Anderson T J, Ansara I. The Ga-In (gallium-indium) system. *Journal of Phase Equilibria*, 1991, 12(1): 64–72
 81. Zhang C, Li L, Yang X, et al. Study on the nucleating agents for gallium to reduce its supercooling. *International Journal of Heat and Mass Transfer*, 2020, 148: 119055
 82. Wang C, Wu H, Chen Z, et al. Self-healing chemistry enables the stable operation of silicon microparticle anodes for high-energy lithium-ion batteries. *Nature Chemistry*, 2013, 5(12): 1042–1048
 83. Mai W, Yu Q, Han C, et al. Self-healing materials for energy-storage devices. *Advanced Functional Materials*, 2020, 30(24): 1909912
 84. Regan M J, Tostmann H, Pershan P S, et al. X-ray study of the oxidation of liquid-gallium surfaces. *Physical Review. B*, 1997, 55(16): 10786–10790
 85. Zavabeti A, Ou J Z, Carey B J, et al. A liquid metal reaction environment for the room-temperature synthesis of atomically thin metal oxides. *Science*, 2017, 358(6361): 332–335
 86. Xu Q, Oudalov N, Guo Q, et al. Effect of oxidation on the mechanical properties of liquid gallium and eutectic gallium-indium. *Physics of Fluids*, 2012, 24(6): 063101
 87. Chen S, Wang H, Sun X, et al. Generalized way to make temperature tunable conductor-insulator transition liquid metal composites in a diverse range. *Materials Horizons*, 2019, 6(9): 1854–1861
 88. Zuraiqi K, Zavabeti A, Allieux F M, et al. Liquid metals in catalysis for energy applications. *Joule*, 2020, 4(11): 2290–2321
 89. Zmic D, Swatik D S. On the resistivity and surface tension of the eutectic alloy of gallium and indium. *Journal of the Less Common Metals*, 1969, 18(1): 67–68
 90. Mott N F. The resistance of liquid metals. *Proceedings of the Royal Society of London. Series A, Containing Papers of a Mathematical and Physical Character*, 1934, 146(857): 465–472
 91. Jeong Y R, Lee G, Park H, et al. Stretchable, skin-attachable electronics with integrated energy storage devices for biosignal monitoring. *Accounts of Chemical Research*, 2019, 52(1): 91–99
 92. Zhang Q, Gao Y, Liu J. Atomized spraying of liquid metal droplets on desired substrate surfaces as a generalized way for ubiquitous printed electronics. *Applied Physics A, Materials Science & Processing*, 2014, 116(3): 1091–1097
 93. Zhang S, Jiang J, Jiang Q, et al. Dynamically conformal mask printing of liquid alloy circuits on morphing objects. *Advanced Materials Technologies*, 2021, 6(6): 2001274
 94. Azadmanjiri J, Thuniki N R, Guzzetta F, et al. Liquid metals-assisted synthesis of scalable 2D nanomaterials: prospective sediment inks for screen-printed energy storage applications. *Advanced Functional Materials*, 2021, 31(17): 2010320
 95. Guo R, Yao S, Sun X, et al. Semi-liquid metal and adhesion-selection enabled rolling and transfer (SMART) printing: a general method towards fast fabrication of flexible electronics. *Science China Materials*, 2019, 62(7): 982–994
 96. Tang L, Mou L, Zhang W, et al. Large-scale fabrication of highly elastic conductors on a broad range of surfaces. *ACS Applied Materials & Interfaces*, 2019, 11(7): 7138–7147
 97. Wu P, Zhou L, Lv S, et al. Self-sintering liquid metal ink with LAPONITE[®] for flexible electronics. *Journal of Materials Chemistry C, Materials for Optical and Electronic Devices*, 2021, 9(9): 3070–3080
 98. Nasreldin M, Mulatier S, Delattre R, et al. Flexible and stretchable microbatteries for wearable technologies. *Advanced Materials Technologies*, 2020, 5(12): 2000412
 99. Wang X, Lu C, Rao W. Liquid metal-based thermal interface materials with a high thermal conductivity for electronic cooling and bioheat-transfer applications. *Applied Thermal Engineering*, 2021, 192: 116937
 100. Lee K T, Jung Y S, Kim T, et al. Liquid gallium electrode confined in porous carbon matrix as anode for lithium secondary batteries. *Electrochemical and Solid-State Letters*, 2008, 11(3): A21
 101. Luo F, Zheng J, Chu G, et al. Self-healing behavior of high capacity metal gallium thin film and powder as anode material for Li-ion battery. *Acta Chimica Sinica*, 2015, 73(8): 808–814 (in Chinese)
 102. Christov S, Rajceva S. Über die abhangigkeit der wasserstoffuberspannung vom aggregatzustand des galliums. *Zeitschrift Fur Elektrochemie*, 1962, 66(6): 484–491
 103. Wen L, Liang J, Chen J, et al. Smart materials and design toward safe and durable lithium ion batteries. *Small Methods*, 2019, 3(11): 1900323
 104. Xu W, Wang J, Ding F, et al. Lithium metal anodes for rechargeable batteries. *Energy & Environmental Science*, 2014, 7

- (2): 513–537
105. Yi L, Liu J. Liquid metal biomaterials: a newly emerging area to tackle modern biomedical challenges. *International Materials Reviews*, 2017, 62(7): 415–440
 106. Liu T, Sen P, Kim C J. Characterization of nontoxic liquid-metal alloy galinstan for applications in microdevices. *Journal of Microelectromechanical Systems*, 2012, 21(2): 443–450
 107. Bernstein L R. Mechanisms of therapeutic activity for gallium. *Pharmacological Reviews*, 1998, 50(4): 665–682
 108. Wang Q, Yu Y, Liu J. Delivery of liquid metal to the target vessels as vascular embolic agent to starve diseased tissues or tumors to death. *Physics (College Park, Md.)*, 2014
 109. Chechetka S A, Yu Y, Zhen X, et al. Light-driven liquid metal nanotransformers for biomedical theranostics. *Nature Communications*, 2017, 8(1): 15432
 110. Sun X, Yuan B, Sheng L, et al. Liquid metal enabled injectable biomedical technologies and applications. *Applied Materials Today*, 2020, 20: 100722
 111. Lu Y, Hu Q, Lin Y, et al. Transformable liquid-metal nanomedicine. *Nature Communications*, 2015, 6(1): 10066
 112. Liu F, Yu Y, Yi L, et al. Liquid metal as reconnection agent for peripheral nerve injury. *Science Bulletin*, 2016, 61(12): 939–947
 113. Nicholas M G, Old C F. Liquid metal embrittlement. *Journal of Materials Science*, 1979, 14(1): 1–18
 114. Trenikhin M V, Bubnov A V, Nizovskii A I, et al. Chemical interaction of the In-Ga eutectic with Al and Al-base alloys. *Inorganic Materials*, 2006, 42(3): 256–260
 115. Senel E, Walmsley J C, Diplas S, et al. Liquid metal embrittlement of aluminium by segregation of trace element gallium. *Corrosion Science*, 2014, 85: 167–173
 116. Nizovskii A I, Belkova S V, Novikov A A, et al. Hydrogen production for fuel cells in reaction of activated aluminum with water. *Procedia Engineering*, 2015, 113: 8–12
 117. Xu S, Cui Y, Yang L, et al. Instant hydrogen production using Ga-In-Sn-Bi alloy-activated Al-water reaction for hydrogen fuel cells. *Journal of Renewable and Sustainable Energy*, 2020, 12(1): 014701
 118. Wang L, Liu J. Liquid metal soft battery and its fabrication method. *China Patent*, CN201510689223.8, 2015
 119. Wang L, Liu J. A room temperature liquid metal battery. *China Patent*, CN201610573221.7, 2016
 120. Liu G, Kim J Y, Wang M, et al. Soft, highly elastic, and discharge-current-controllable eutectic gallium-indium liquid metal-air battery operated at room temperature. *Advanced Energy Materials*, 2018, 8(16): 1703652
 121. Gao J, Ye J, Chen S, et al. Liquid metal foaming via decomposition agents. *ACS Applied Materials & Interfaces*, 2021, 13(14): 17093–17103
 122. Guo X, Ding Y, Xue L, et al. A self-healing room-temperature liquid-metal anode for alkali-ion batteries. *Advanced Functional Materials*, 2018, 28(46): 1804649
 123. Liu D, Su L, Liao J, et al. Rechargeable soft-matter EGaIn-MnO₂ battery for stretchable electronics. *Advanced Energy Materials*, 2019, 9(46): 1902798
 124. Wei S, Liu H, Wei R, et al. Cathodes with MnO₂ catalysts for metal fuel battery. *Frontiers in Energy*, 2019, 13(1): 9–15
 125. MacFarlane D R, Pringle J M, Howlett P C, et al. Ionic liquids and reactions at the electrochemical interface. *Physical Chemistry Chemical Physics*, 2010, 12(8): 1659–1669
 126. Liu F J, Yu Y Z, Wang L, et al. 3D printing of flexible room-temperature liquid metal battery. 2017, arxiv:1802.01655
 127. Fu H, Liu G, Xiong L, et al. A shape-variable, low-temperature liquid metal-conductive polymer aqueous secondary battery. *Advanced Functional Materials*, 2021, 31(50): 2107062
 128. Wang K, Hu J, Chen T, et al. A high-performance room-temperature Li||Ga-Sn liquid metal battery for grid energy storage. *Energy Technology (Weinheim)*, 2021, 9(9): 2100330
 129. Cao Z, Zhang Y, Cui Y, et al. Harnessing the unique features of 2D materials toward dendrite-free metal anodes. *Energy and Environmental Materials*, 2021: 1–23
 130. Zhao L, Sottos N R. Autonomous strategies for improved performance and reliability of Li-ion batteries. *Advanced Energy Materials*, 2021, 11(5): 2003139
 131. Liu S, Zhao Q, Zhang X, et al. A high rate and long cycling life lithium metal anode with a self-repairing alloy coating. *Journal of Materials Chemistry A, Materials for Energy and Sustainability*, 2020, 8(34): 17415–17419
 132. Liu J, Zhang J, Yang Z, et al. Materials science and materials chemistry for large scale electrochemical energy storage: from transportation to electrical grid. *Advanced Functional Materials*, 2013, 23(8): 929–946
 133. Zhang Q, Wu L, Fan M, et al. A room temperature alloying strategy to enable commercial metal foil for efficient Li/Na storage and deposition. *Energy Storage Materials*, 2021, 34: 708–715
 134. Zhang G, Deng H, Tao R, et al. Constructing a liquid-metal based self-healing artificial solid electrolyte interface layer for Li metal anode protection in lithium metal battery. *Materials Letters*, 2020, 262: 127194
 135. Wei C, Fei H, An Y, et al. Uniform Li deposition by regulating the initial nucleation barrier via a simple liquid-metal coating for a dendrite-free Li-metal anode. *Journal of Materials Chemistry A, Materials for Energy and Sustainability*, 2019, 7(32): 18861–18870
 136. Wei C, Fei H, Tian Y, et al. Isotropic Li nucleation and growth achieved by an amorphous liquid metal nucleation seed on MXene framework for dendrite-free Li metal anode. *Energy Storage Materials*, 2020, 26: 223–233
 137. Wei C, Tan L, Tao Y, et al. Interfacial passivation by room-temperature liquid metal enabling stable 5 V-class lithium-metal batteries in commercial carbonate-based electrolyte. *Energy Storage Materials*, 2021, 34: 12–21
 138. Ding Y, Guo X, Yu G. Next-generation liquid metal batteries based on the chemistry of fusible alloys. *ACS Central Science*, 2020, 6(8): 1355–1366
 139. Okamoto H. Ga-Li (gallium-lithium). *Journal of Phase Equilibria*, 1999, 20(1): 92
 140. Chan C K, Peng H, Liu G, et al. High-performance lithium battery anodes using silicon nanowires. *Nature Nanotechnology*, 2008, 3(1): 31–35
 141. Laforge B, Levan-Jodin L, Salot R, et al. Study of germanium as electrode in thin-film battery. *Journal of the Electrochemical Society*, 2008, 155(2): A181

142. Winter M, Besenhard J O. Electrochemical lithiation of tin and tin-based intermetallics and composites. *Electrochimica Acta*, 1999, 45(1–2): 31–50
143. Han B, Yang Y, Shi X, et al. Spontaneous repairing liquid metal/Si nanocomposite as a smart conductive-additive-free anode for lithium-ion battery. *Nano Energy*, 2018, 50: 359–366
144. Ma L, Schroeder M A, Borodin O, et al. Realizing high zinc reversibility in rechargeable batteries. *Nature Energy*, 2020, 5(10): 743–749
145. Xu C, Li B, Du H, et al. Energetic zinc ion chemistry: the rechargeable zinc ion battery. *Angewandte Chemie International Edition*, 2012, 51(4): 933–935
146. Liu C, Luo Z, Deng W, et al. Liquid alloy interlayer for aqueous zinc-ion battery. *ACS Energy Letters*, 2021, 6(2): 675–683
147. Blanc L E, Kundu D, Nazar L F. Scientific challenges for the implementation of Zn-ion batteries. *Joule*, 2020, 4(4): 771–799
148. Lin M, Gong M, Lu B, et al. An ultrafast rechargeable aluminium-ion battery. *Nature*, 2015, 520(7547): 324–328
149. Jiao H, Jiao S, Li S, et al. Liquid gallium as long cycle life and recyclable negative electrode for Al-ion batteries. *Chemical Engineering Journal*, 2020, 391: 123594
150. Hapuarachchi S N S, Nerkar J Y, Wasalathilake K C, et al. Utilizing room temperature liquid metals for mechanically robust silicon anodes in lithium-ion batteries. *Batteries & Supercaps*, 2018, 1(3): 122–128
151. Wu Y, Huang X, Huang L, et al. Self-healing liquid metal and Si composite as a high-performance anode for lithium-ion batteries. *ACS Applied Energy Materials*, 2018, 1(4): 1395–1399
152. Wang J, Wang L, Ma Y, et al. Liquid gallium encapsulated in carbon nanofibers for high performance lithium storage. *Materials Letters*, 2018, 228: 297–300
153. Shi Y, Song M, Zhang Y, et al. A self-healing CuGa₂ anode for high-performance Li ion batteries. *Journal of Power Sources*, 2019, 437: 226889
154. Zhu J, Wu Y, Huang X, et al. Self-healing liquid metal nanoparticles encapsulated in hollow carbon fibers as a free-standing anode for lithium-ion batteries. *Nano Energy*, 2019, 62: 883–889
155. Wei C, Fei H, Tian Y, et al. Room-temperature liquid metal confined in MXene paper as a flexible, freestanding, and binder-free anode for next-generation lithium-ion batteries. *Small*, 2019, 15(46): 1903214
156. Li T, Cui Y, Fan L, et al. A self-healing liquid metal anode with PEO-Based polymer electrolytes for rechargeable lithium batteries. *Applied Materials Today*, 2020, 21: 100802
157. Hapuarachchi S N S, Wasalathilake K C, Siriwardena D P, et al. Interfacial engineering with liquid metal for Si-based hybrid electrodes in lithium-ion batteries. *ACS Applied Energy Materials*, 2020, 3(6): 5147–5152
158. Yang Y, Hao J, Xue J, et al. Morphology regulation of Ga particles from ionic liquids and their lithium storage properties. *New Journal of Chemistry*, 2021, 45(9): 4408–4413
159. Park M, Kim H J, Jeong I, et al. Mechanically recoverable and highly efficient perovskite solar cells: investigation of intrinsic flexibility of organic-inorganic perovskite. *Advanced Energy Materials*, 2015, 5(22): 1501406
160. Pasquier A D, Miller S, Chhowalla M. On the use of Ga-In eutectic and halogen light source for testing P3HT-PCBM organic solar cells. *Solar Energy Materials and Solar Cells*, 2006, 90(12): 1828–1839
161. Ongul F, Yuksel S A, Bozar S, et al. Vacuum-free processed bulk heterojunction solar cells with E-GaIn cathode as an alternative to Al electrode. *Journal of Physics D, Applied Physics*, 2015, 48(17): 175102
162. Pham V T H, Trinh T K, Truong N T N, et al. Liquid eutectic GaIn as an alternative electrode for PTB7: PCBM organic solar cells. *Japanese Journal of Applied Physics*, 2017, 56(4): 046501
163. Savagatrup S, Printz A D, O'Connor T F, et al. Efficient characterization of bulk heterojunction films by mapping gradients by reversible contact with liquid metal top electrodes. *Chemistry of Materials*, 2017, 29(1): 389–398
164. Dai D, Liu J, Zhou Y. Harvesting biomechanical energy in the walking by shoe based on liquid metal magnetohydrodynamics. *Frontiers in Energy*, 2012, 6(2): 112–121
165. Dai D, Zhou Y, Liu J. Liquid metal based thermoelectric generation system for waste heat recovery. *Renewable Energy*, 2011, 36(12): 3530–3536
166. Xiang S, Liu D, Jiang C, et al. Liquid-metal-based dynamic thermoregulating and self-powered electronic skin. *Advanced Functional Materials*, 2021, 31(26): 2100940
167. Tang W, Jiang T, Fan F, et al. Liquid-metal electrode for high-performance triboelectric nanogenerator at an instantaneous energy conversion efficiency of 70.6%. *Advanced Functional Materials*, 2015, 25(24): 3718–3725
168. Padmanabhan Ramesh V, Sargolzaeiaval Y, Neumann T, et al. Flexible thermoelectric generator with liquid metal interconnects and low thermal conductivity silicone filler. *npj Flexible Electronics*, 2021, 5(1): 5
169. Zadan M, Malakooti M H, Majidi C. Soft and stretchable thermoelectric generators enabled by liquid metal elastomer composites. *ACS Applied Materials & Interfaces*, 2020, 12(15): 17921–17928
170. Zhang J, Liu M, Pearce G, et al. Strain stiffening and positive piezoconductive effect of liquid metal/elastomer soft composites. *Composites Science and Technology*, 2021, 201: 108497
171. Yu L, Wang L, Wu D, et al. Enhanced piezoelectric performance of electrospun PVDF nanofibers with liquid metal electrodes. *ECS Journal of Solid State Science and Technology: JSS*, 2018, 7(9): N128–N131
172. Zi Y, Niu S, Wang J, et al. Standards and figure-of-merits for quantifying the performance of triboelectric nanogenerators. *Nature Communications*, 2015, 6(1): 8376
173. Li X, Tao J, Zhu J, et al. A nanowire based triboelectric nanogenerator for harvesting water wave energy and its applications. *APL Materials*, 2017, 5(7): 074104
174. Yang Y, Sun N, Wen Z, et al. Liquid-metal-based super-stretchable and structure-designable triboelectric nanogenerator for wearable electronics. *ACS Nano*, 2018, 12(2): 2027–2034
175. Dubal D P, Chodankar N R, Kim D H, et al. Towards flexible solid-state supercapacitors for smart and wearable electronics. *Chemical Society Reviews*, 2018, 47(6): 2065–2129
176. So J H, Koo H J. Study on the electrochemical characteristics of a

- EGaIn liquid metal electrode for supercapacitor applications. *Transactions of the Korean Hydrogen and New Energy Society*, 2016, 27(2): 176–181
177. Chen J, Lee P S. Electrochemical supercapacitors: from mechanism understanding to multifunctional applications. *Advanced Energy Materials*, 2021, 11(6): 2003311
178. Park H, Song C, Jin S W, et al. High performance flexible micro-supercapacitor for powering a vertically integrated skin-attachable strain sensor on a bio-inspired adhesive. *Nano Energy*, 2021, 83: 105837
179. Liu L, Niu Z, Zhang L, et al. Nanostructured graphene composite papers for highly flexible and foldable supercapacitors. *Advanced Materials*, 2014, 26(28): 4855–4862
180. Zhang L, Liu D, Wu Z, et al. Micro-supercapacitors powered integrated system for flexible electronics. *Energy Storage Materials*, 2020, 32: 402–417